Physical processes in the solar atmosphere associated with flares

B. V. Somov and S. I. Syrovatskiĭ

P. N. Lebedev Physics Institute, USSR Academy of Sciences
Usp. Fiz. Nauk **120**, 217–257 (October 1976)

Flares on the sun release an enormous amount of energy in the form of accelerated particles, heat fluxes, matter fluxes, and radiation. The relative importance of each of these energy channels is reviewed and the reaction of the solar atmosphere to the corresponding energy fluxes is considered. The possibility of determining the characteristics of the primary process of the flare from its secondary manifestations in the atmosphere of the sun is discussed.

PACS numbers: 96.20.Sh

CONTENTS

1. INTRODUCTION

A. Main observational manifestations and energy budget of solar flares

Solar flares have long attracted the interest of observers and theoreticians for many reasons, above all because flares are the most powerful manifestations of activity of the Sun that influence the state of the Earth's atmosphere and cislunar space.[1–5] A second and hardly less important reason is that, in contrast to flares on other stars and also many other nonstationary phenomena in the universe similar to solar flares, the latter are accessible to comprehensive study. The emission of solar flares is observed in virtually the entire electromagnetic spectrum from kilometer wavelengths to hard gamma rays by means of terrestrial, satellite, and interplanetary observatories. Simultaneously, one can directly detect particles accelerated in flares, plasma ejected into interplanetary space, shock waves, and also secondary ionospheric and geomagnetic effects. As a result, the observations of solar flares, especially in recent years (see, for example, [6]) have a very comprehensive nature, which enables one to obtain very detailed information about the physical processes taking place in the flares.

The main phenomenon in a solar flare is the rapid release of an enormous energy. In large flares, it reaches 10^{32} erg in a time of about 10^3 sec, which corresponds to a mean power 10^{29} erg/sec during this period. It is probable that the power may be several times larger at certain times. A very important feature of flares is the fact that an appreciable and sometimes possibly the main part of this energy is released in nonthermal forms: in accelerated particles, in the form of ejections of matter, and in hard electromagnetic radiation. This makes the study of solar flares particularly interesting in connection with the general problem of the generation of energetic particles and cosmic rays.[7]

Table I contains typical values of the total energy $\mathscr{E}$ (erg) and the power $\mathscr{F}$ (erg/sec) released in different channels for flares of different power. We have here used the data of various sources, in particular[6].

The main task of the theory of solar flares is to explain this very large power of the energy and its nonthermal character. At the present time, the most probable mechanism of solar flares must be regarded as the process of formation and explosive breakup (for brevity, we shall call it explosion) of a current sheet in the plasma in the region of strong magnetic fields ([8], see also[9]). Investigations of this and other processes in neutral current sheets in a plasma have as their aim the elucidation of the possibility and efficiency of conversion of magnetic energy of the current into other forms, in particular the energy of accelerated particles. Such investigations are currently being carried intensively by analytic,[8,10–15] numerical,[16–21] and experimental[22–29] methods, both here in the Soviet Union and abroad.

The observation of pre-flare current sheets on the Sun could have fundamental importance for the problem of predicting solar flares. However, the practical possibilities of such observations and their interpretation have been clarified only recently.[30] On the other hand, the energy liberated in a flare gives rise to numerous secondary processes in the Sun's atmosphere, and it is they that form the basis of the complicated observed picture of the flare. Therefore, from the point of view of the interpretation of the observations, the theory of the effect of the primary flare process on the atmosphere of the Sun is of great importance. The main

TABLE I. Energy budget of solar flares.

Form in which energy is released	Most powerful flares $\mathscr{E}$, erg	Most powerful flares $\mathscr{F}$, erg/sec	Subflares $\mathscr{E}$, erg	Subflares $\mathscr{F}$, erg/sec
Radiation:				
ultraviolet	$(3-5)\cdot 10^{31}$	$(3-5)\cdot 10^{28}$	$(3-5)\cdot 10^{29}$	$(3-5)\cdot 10^{27}$
soft x rays	10^{31}	$3\cdot 10^{27}$	10^{29}	10^{27}
optical, continuum	$(1-3)\cdot 10^{30}$	$3\cdot 10^{27}$	?	?
in the line H_α	10^{30}	$3\cdot 10^{26}$	10^{26}	$3\cdot 10^{23}$
hard x rays	$(3-5)\cdot 10^{26}$	$(3-5)\cdot 10^{23}$	$(3-5)^{*)}\cdot 10^{24}$	$(3-5)\cdot 10^{22}$
gamma	$(3-5)\cdot 10^{25}$	$(3-5)\cdot 10^{22}$	...	...
radio	10^{24}	10^{21}	10^{22}	10^{20}
Energetic particles in interplanetary space:				
electrons (>20 keV)	10^{29}	10^{26}	10^{27}	10^{25}
protons (>10 MeV)	$\sim 2\cdot 10^{31}$	10^{28}	...?	...?
Gas dynamic motions (ejections) above the chromosphere	$\sim 3\cdot 10^{31}$	10^{29}	10^{29}	10^{26}
Interplanetary shock waves	$\sim 10^{32}$		...	...
Total	$(1-2)\cdot 10^{32}$	$(1-2)\cdot 10^{29}$	$(4-6)\cdot 10^{29}$	$(4-6)\cdot 10^{27}$

*)Absent for the overwhelming majority of subflares.

task of such a theory is to elucidate the properties of the flare mechanism from the observed manifestations of the secondary processes. It is clear that such a problem is complicated, not always unambiguous, and that one can begin to solve it only by studying the individual elementary physical processes in the atmosphere of the Sun corresponding to a particular energy release channel in the principal flare process.

Below, we shall not discuss the fundamental questions relating to the dynamics of the current sheet (those interested are referred to the reviews[8-9]) or the possibility of observing current sheets on the Sun.[30] Our main attention will be concentrated on the secondary processes due to the liberation of energy in the current sheet. We point out directly that the observed complexity and variety of solar flares evidently precludes the possibility of regarding their mechanism as a process in which individual flares differ only in their strength. In reality, flares also differ in their space-time structure and the relative role of the different energy release channels. Nevertheless, the review below of results shows that the process of formation and breakup of a current sheet in the plasma in a strong magnetic field can provide a basis for all the observed manifestations of a flare.

B. Current sheet in the plasma as origin and source of the energy of a solar flare. Stage of development of the current sheet and energy release channels

Usually, solar flares arise in a region of strong magnetic fields in the so-called active regions on the surface of the Sun, which, as a rule, contain sun spots. Observational data and theoretical arguments indicate that the main flare process is due to the accumulation of free magnetic energy in the upper chromosphere and corona. By "free" we here mean excess magnetic energy compared with the energy of a potential field having the same sources on the photosphere. In other words, the free magnetic energy of an active region is associated with currents flowing in the solar atmosphere above the level of the photosphere. Such an excess can arise in different ways. One of them is, for example, the following. The potential magnetic field varies because of the subphotospheric motion of its sources. At a certain time, it may become fairly complicated. For example, the number of field sources becomes greater than three. Then this field will contain a so-called limiting line of force.[31] It is an important topological feature of the field since it is a line of force common to several independent magnetic fluxes. The magnetic flux needed if the magnetic field is to remain a potential field despite the motion of its sources is transported through this line.[32,33] In the presence of plasma, a limiting line of force plays the same role as a singular line of force of the magnetic field, which has been well studied in two-dimensional problems.[8-9] Namely, as soon as a limiting line appears, the electric field that is induced by the changes of the magnetic field gives rise to a current along the limiting line of force. This current, because of the interaction with the magnetic field, takes the form of a current sheet and, under the conditions of high conductivity of the solar plasma, prevents a redistribution of the magnetic fluxes. As a result, there is an accumulation of energy in the form of the magnetic energy of the current sheet in the upper chromosphere and corona.

Below, we shall assume known the properties of the neutral current sheet in the plasma in the region of strong magnetic fields as the assumed energy source of the flare. In particular, we shall distinguish three main stages in the development of the current sheet[8,10] and bring them into correspondence with the three phases of a solar flare.[34,35]

The initial phase is the comparatively long (hours or tens of hours) stage of the formation and extension of the current sheet. During this stage, the mechanism of Coulomb heating of the plasma by the strong current in the sheet is predominant. In principle, a stationary

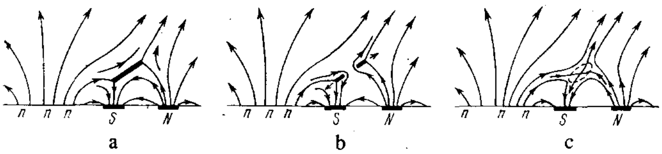

FIG. 1. Stages in the development of a current sheet in the atmosphere of the Sun in the region of a strong magnetic field: quasistationary pre-flare current sheet (a), breaking of the current sheet—the explosive phase of the flare (b), and the quasistationary reconnection of the lines of force in the region of anomalous resistance—the hot phase of the flare (c).

regime can be established when the current sheet has extended so far that the rate of dissipation of the magnetic field in it halts a further growth of the magnetic energy. It is interesting that under the conditions of the solar atmosphere the temperature of such a quasistationary sheet is determined by the balance of Joule heating and cooling by emission.[30] Under definite conditions, this balance becomes impossible and the essentially nonstationary stage in the development of the current sheet begins.

The most interesting phase in the flare is the explosive phase, when the tremendous amount of energy stored in the magnetic field of the sheet is set free in a short time (seconds or tens of seconds). This energy is liberated in three principal forms: hydrodynamic motions (disruption of the sheet accompanied by rapid motions of plasma), thermal heating as a result of anomalous resistance in the region of breakup of the current sheet, and, finally, in the form of accelerated particles (electrons, protons, and nuclei of heavier elements).

The third, hot phase of the flare corresponds to the stage when there exists a hot coronal region. Here the principal energy release channel is apparently turbulent heating.

As an example, Fig. 1 shows the stages in the development of a current sheet in the atmosphere of the Sun in the region of a strong magnetic field produced by a bipolar sun spot group (N and S) and a background field of one polarity (n).

In this review, we shall mainly discuss the mechanisms of heating of the solar atmosphere during the explosive (or flash) phase and the observational consequences of each of the main energy release channels corresponding to them. Specifically, we shall consider the following processes: heating by thermal fluxes and energetic particles, heating by the emission of the hot region, ejections, and gas dynamic heating of the plasma.

C. General formulation of the problem of the effect of flares on the solar atmosphere

The diversity of physical processes caused by a flare in the solar atmosphere is due to the existence of several energy release channels (heat, accelerated particles, radiation, gas dynamic flows), the difference between the powers and characteristic times of these channels, and also many other factors: the height of the energy source, the configuration of the magnetic field, the initial and boundary conditions, etc. At the same time, many of the secondary processes have common features; for example, many are characterized by local heating of the atmosphere to high temperatures, radiative cooling of the hot region, and its gas dynamical expansion.

The heating of the atmosphere by the heat flux is characterized by the power

$$\mathcal{P}_e(n, T) = \operatorname{div}(\varkappa \nabla T) \ (\mathrm{erg \cdot cm^{-3} \cdot sec^{-1}}), \qquad (1.1)$$

and in the upper chromosphere and corona is determined by the electron heat conductivity

$$\varkappa = \varkappa_e \approx 1.8 \cdot 10^{-5} \lambda^{-1} T^{5/2}; \qquad (1.2)$$

where λ is the Coulomb logarithm and n and T are the concentration of the plasma and its temperature. In the region of the strong magnetic field, the heat flux is along the lines of force. At low temperatures ($T \lesssim 10^4$ °K) the thermal conductivity of neutral atoms $\varkappa_H$ becomes important and the heat flux becomes isotropic (see[36] for more details).

Below, we shall ignore the inhomogeneity of the magnetic tubes—the dependence of the tube cross sectional area S on the coordinate s along the tube—although for some phenomena this inhomogeneity may have decisive importance. Thus, we shall consider one-dimensional problems. In this case, as is well known, it is convenient to use a "Lagrangian" variable:

$$\xi = \int_0^s n(s)\, ds \ (\mathrm{cm^{-2}}), \qquad (1.3)$$

which is the thickness of matter along a tube of unit cross section.

The heating by electrons accelerated in the flare is due to Coulomb energy losses in the plasma and is proportional to the plasma concentration:

$$\mathcal{P}_c(n, \xi) = nP(\xi) \ (\mathrm{erg \cdot cm^{-3} \cdot sec^{-1}}). \qquad (1.4)$$

The heating of the atmosphere of the Sun by energetic electrons and protons with a power-law spectrum will be discussed in Chap. 3.

The cooling of the hot plasma by emission in the approximation of a transparent medium and impact excitation by thermal electrons is of the form

$$\mathcal{L}(n, T) = nn_e L(T) \ (\mathrm{erg \cdot cm^{-3} \cdot sec^{-1}}), \qquad (1.5)$$

where n_e is the electron density. In the opposite limiting case, absorption of external radiation is of fundamental importance and therefore heating by radiation (Chap. 5):

$$\mathcal{P}_r(\xi) = \operatorname{div} \int F_\nu(0) \exp(-\sigma_\nu \xi)\, d\nu \ (\mathrm{erg \cdot cm^{-3} \cdot sec^{-1}}). \qquad (1.6)$$

Here, $F_\nu(0)$ is the spectrum of the radiative energy flux at the boundary $\xi = 0$ of the heated region and σ_ν is the frequency-dependent coefficient of true absorption of photons.

In fast processes in the flare plasma (strong electric field), impulsive heating by energetic electrons, instability of thermal equilibrium, etc. the difference between the electron T_e and ion T_i temperatures may be important. The rate of exchange of energy between the electron and ion components is[36]

$$Q(n, T_e, T_i) \approx 4.8 \cdot 10^{-27} n^2 \lambda (T_e - T_i) T_e^{-3/2} \ (\mathrm{erg \cdot cm^{-3} \cdot sec^{-1}}). \qquad (1.7)$$

On the other hand, in the region of large velocity gradients, viscous heating of the ions is important:

$$\mathcal{P}_v(n, T_i, v) = \frac{4}{3} \eta_i n^2 \left(\frac{\partial v}{\partial \xi}\right)^2 \ (\mathrm{erg \cdot cm^{-3} \cdot sec^{-1}}), \qquad (1.8)$$

where $\eta_i(T_i)$ is the ion viscosity.[36]

Therefore, we shall treat the plasma flows associated with a flare in the hydrodynamic but two-temperature approximation (see, for example, [37]) and we write the corresponding system of equations in terms of the Lagrangian variable ξ:

$$\frac{\partial n}{\partial t} + n^2 \frac{\partial v}{\partial \xi} = 0, \qquad (1.9)$$

$$\frac{\partial v}{\partial t} + \frac{1}{m_{\mathrm{H}}} \frac{\partial}{\partial \xi} [nk(T_e + T_i)] = \frac{4}{3} \frac{1}{m_{\mathrm{H}}} \frac{\partial}{\partial \xi} \left(\eta_i n \frac{\partial v}{\partial \xi}\right) + g_\odot \cos\psi, \qquad (1.10)$$

$$\frac{nk}{(\gamma-1)} \frac{\partial T_e}{\partial t} - kT_e \frac{\partial n}{\partial t} = \mathcal{P}_c(n, T_e) + \mathcal{P}_e(n, \xi) + \mathcal{P}_r(\xi) - \mathcal{L}(n, T_e) - Q(n, T_e, T_i), \qquad (1.11)$$

$$\frac{nk}{(\gamma-1)} \frac{\partial T_i}{\partial t} - kT_i \frac{\partial n}{\partial t} = \mathcal{P}_v(n, T_i, v) + Q(n, T_e, T_i); \qquad (1.12)$$

where $g_\odot$ is the acceleration due to gravity on the Sun, ψ is the angle between this force and the direction of motion of the plasma, γ is the ratio of the specific heats, and m_{H} is the mass of the hydrogen atom.

Augmented by the necessary initial and boundary conditions, the system of equations (1.9)–(1.12) enables one to investigate many phenomena in the corona and chromosphere due to a solar flare. However, even this one-dimensional system is fairly complicated and one must begin such an investigation by considering special solutions of the system corresponding to individual heating and cooling mechanisms under particular conditions and simplifying assumptions. In this way, one can establish the efficiency of the particular mechanisms of flare heating, establish the specific observable manifestations of the individual physical processes in the solar atmosphere caused by flares, and their position in the complicated observed picture of a solar flare.

2. HEATING OF THE SOLAR ATMOSPHERE BY HEAT FLUXES

A. Role of electron heat conduction in the atmosphere of the sun

It is well known that the electron thermal conductivity (1.2) guarantees a rapid equalization of the temperature in the corona, making the corona isothermal along tubes of magnetic lines of force.[1,2] Korchak and Platov[38] were the first to draw attention to the high efficiency of electron heat conduction as the mechanism of cooling of the plasma heated in the flare. In[39], Culhane, Vesecky, and Phillips analyzed, besides thermal conduction, cooling of the electron component of a nonisothermal plasma by Coulomb collisions with the ions (1.7) and showed that this mechanism rapidly equalizes the electron and ion temperatures. In addition, they showed that the cooling of the high-temperature region by emission (1.5) may be comparable with the heat conduction cooling. With certain simplifying assumptions (basically, by the introduction of an effective size), expressions were obtained in[38,39] for the characteristic time of cooling of the flare plasma by heat conduction.

It is also known that in the absence of flares the reverse heat flux from the corona into the chromosphere creates a transition layer between them. However, here the heat flux is small and is not the main heating mechanism of the chromosphere.

B. Stationary heating of the atmosphere by heat conduction

In connection with flares, the problem of the stationary heating of the Sun's atmosphere by a heat flux was solved by Syrovatskiĭ and Shmeleva.[40,41] They considered the heat flux along an isolated magnetic tube whose lower end is immersed in the chromosphere at a certain depth, where the concentration and temperature of the unperturbed plasma are n_∞ and T_∞ (Fig. 2). The upper end of the tube is in the corona and kept at a certain constant temperature T_0 by a constant flux F_0 of thermal energy. As a result, there is established a temperature distribution over the thickness of the matter that ensures at every point a balance between the heating by the heat flux and the radiation losses. This distribution is determined by the stationary form of the energy equation (1.11) in the absence of motions of the plasma and nonthermal heating:

$$\frac{d}{d\xi}\left(\varkappa n \frac{dT}{d\xi}\right) + \frac{1}{n} \mathcal{P}_\infty(T_\infty, n_\infty) = L(T) n_e; \qquad (2.1)$$

here, $\mathcal{P}_\infty(T_\infty, n_\infty)$ is the part of the heating power due to the external sources that maintain the initial temperature $T_\infty(\xi)$ in the chromosphere.

The steady-state temperature distribution is shown schematically in Fig. 3. It is characterized by the presence of a hot region, a thin transition layer, and a low-temperature region; these emit mainly in the soft x-ray, ultraviolet, and optical ranges, respectively. It is characteristic that the main part of the energy is radiated in the ultraviolet and soft x-ray ranges in the transition layer and the high-temperature region; only

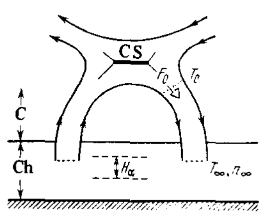

FIG. 2. Current sheet (CS) as energy source for heating of the corona (C) and chromosphere (Ch) by heat flux (F_0) along tubes of magnetic lines of force. T_0 is the temperature corresponding to the boundary energy flux F_0 at the upper end of the magnetic tube; T_∞ and n_∞ are the temperature and concentration at the cold lower end of the tube.

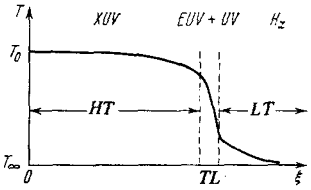

FIG. 3. Distribution of the temperature T with respect to the thickness of matter ξ along an isolated magnetic tube. The high-temperature region (HT) is the source of x-ray and extreme ultraviolet radiation (XUV); the low-temperature region (LT), of the visible optical emission; the thin transition layer (TL) emits mainly in the ultraviolet (EUV+UV) region.

a slight amount (about 1%) of the original heat flux is emitted in optical lines of the visible spectrum (predominantly in H_α).

An important feature of the stationary thermal heating is that in the hot region and in the transition layer the temperature distribution has a universal nature, i.e., it is determined by some function of the dimensionless thickness ξ (see Fig. 4 in[41]), and the form of this function depends only on the assumption whether the gas pressure succeeds in being equalized along the tube or whether, conversely, the initial distribution of the plasma density remains unchanged. In the case of solar flares, these two limiting heating regimes are realized depending on the ratio between the characteristic heating time t_h and the characteristic pressure equalization time t_p. If it is assumed that in the case of vertical heating of the chromosphere t_p is comparable with the time of propagation of acoustic disturbances in the scale height $h_0 = kT_\infty/mg_\odot$, i.e., in the scale that characterizes the inhomogeneity of the initial density distribution, then $t_p \approx 15$–20 sec for typical chromospheric temperatures.

If

$$t_h \gg t_p, \tag{2.2}$$

then the density can be redistributed during the heating process and a heating regime with $p = \text{const}$ is realized. Conversely, if the heating occurs so rapidly that

$$t_h \ll t_p, \tag{2.3}$$

the distribution of the density remains unchanged and practically uniform ($n = \text{const}$) for the range of temperatures corresponding to the transition layer since the thickness of the transition layer is, according to the calculations of[40,41], much less than h_0.

In[42] Shmeleva and Syrovatskiĭ compared the theoretical calculations of[40] and[41] with the data of the first ultraviolet observations[43,44] with the aim of determining which of the heating regimes is realized in a flare. It was found that for subflares, the temperature range $T \gtrsim 10^5$ °K is described better by the model of rapid heating. Evidence in favor of rapid heating of the solar atmosphere during the explosive phase of certain impulsive flares, for example, the flare on August 2, 1972 at 1838 UT, is also provided by the analysis of the x-

TABLE II. Flare heating of the chromosphere by heat fluxes and energetic electrons.

Heat fluxes					Energetic electrons				
T_0, 10^7 °K	ξ, cm^{-2}	n_H, cm^{-3}	$F_c(0)$, erg·cm^{-2}·sec^{-1}	$F_c(\xi)/F_c(0)$, %	$F(\xi)/F(0)$, %: $\gamma=6$	$\gamma=5$	$\gamma=4$	$\gamma=3$	E_0, keV
				a) $p = \text{const}$					
1	$8.7\cdot10^{19}$	$5\cdot10^{12}$	$3\cdot10^{7}$	1.5	2.0	5.0	13	34	23
2	$3.8\cdot10^{20}$	$2\cdot10^{13}$	$2\cdot10^{8}$	1.2	0.1	0.53	2.9	16	48
3	$9.0\cdot10^{20}$	$8\cdot10^{13}$	$9\cdot10^{8}$	1.0	0.02	0.15	1.2	11	73
				b) $n = \text{const}$					
1	$2.2\cdot10^{20}$	10^{13}	$9\cdot10^{10}$	$3.8\cdot10^{-3}$	0.3	1.2	5.0	21	37
2	$9.3\cdot10^{20}$	$8\cdot10^{13}$	$2\cdot10^{12}$	$1.4\cdot10^{-3}$	$1.7\cdot10^{-2}$	0.14	1.2	10	75
3	$2.0\cdot10^{21}$	$2\cdot10^{14}$	$6\cdot10^{12}$	$7.0\cdot10^{-4}$	$4.0\cdot10^{-3}$	0.05	0.55	7.1	110

ray data. This is discussed below in connection with the heating of the solar atmosphere by the emission of the hot flare plasma.[45] However, for a final conclusion about this question more detailed data on the x-ray and ultraviolet emission of individual flares are needed.

An important difference between these limiting heating regimes is that at one and the same boundary temperature T_0 in the case of rapid heating with $n = \text{const}$ a much greater flux F_0 of thermal energy is required than in the case $p = \text{const}$. This effect is shown in Fig. 4, in which the boundary heat flux F_0, measured in units of

$$F_\infty \approx (1.0 - 1.2)\cdot10^{-9} n_\infty \text{ (erg}\cdot\text{cm}^{-2}\cdot\text{sec}^{-1}\text{)}, \tag{2.4}$$

for $n_\infty = 10^{11}$–10^{15} cm^{-3}, is represented as a function of the boundary temperature T_0 (see Fig. 2 and Table II in[46]).

C. Thermal heating during the initial phase of a flare

Švestka[46] has suggested a number of observational arguments that for the majority of chromospheric flares the heat conduction heating mechanism is the only one during the initial phase of the flare. According to the theory,[8,9,30] the power liberated during the first phase in the form of heat can be estimated in the approximation of a stationary current sheet and may reach about 10^{28} erg/sec. This power is sufficient for stationary heating of the current sheet to temperatures not exceeding $8\cdot10^4$ °K. At these temperatures, radiative losses equalize Joule heating, and removal of energy by the plasma flux and heat conduction play a secondary role.[30] Therefore, the main part of the power is emit-

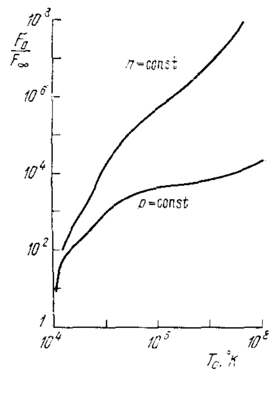

FIG. 4. Boundary flux F_0 of the thermal energy as a function of the boundary temperature T_0 in opposite limiting heating regimes: fast heating ($n = \text{const}$) and slow heating ($p = \text{const}$).

ted in the ultraviolet lines present in the ordinary transition layer between the corona and chromosphere. Enhanced emission in these lines is observed in bright compact points near the zero line of the photospheric magnetic field. According to[47], it is this situation that precedes the explosive phase of the flare.

We mention here that the balance noted above refers to a stationary current sheet. During the formation of the sheet, the energy balance in it may be different, and this may be manifested in a higher temperature of the current sheet and the plasma surrounding it.

D. Explosive phase of the flare and the thermal heating

The explosive (or flash) phase is the most powerful stage of the flare process. It is manifested at all levels of the solar atmosphere from the lower chromosphere, where the optical continuum is formed (white-light flare), to the outer corona, where powerful shock waves and energetic particles reach. The emission during the explosive phase of large flares encompasses the entire electromagnetic spectrum from long radiowaves to hard x and gamma rays.

According to the x-ray and ultraviolet observations (see, for example, [48–53]) a hot coronal region with observed temperatures up to $(1-3)\cdot 10^7$ °K is formed during the explosive phase. In a quasistationary regime, such a temperature corresponds to heating of the chromosphere to a thickness ξ cm^{-2}. Here, the thickness ξ is measured vertically into the chromosphere from its upper boundary (transition layer) in the quiet atmosphere to the low-temperature region of the flare (Fig. 5). The corresponding values of ξ are calculated in the two limiting cases: a) $p = \text{const}$ and b) $n = \text{const}$ and are given in the second column of Table II. In the third column, the hydrogen concentrations in the low-temperature region are given. From these values, the energy flux units (2.4) are calculated and, by means of Fig. 4, the boundary fluxes F_0 of thermal energy determined. They are given in the fourth column of Table II.

In the case $p = \text{const}$, the fraction of the heat flux that penetrates below the flare transition layer into the low-temperature optical region of the flare (given in the fifth column of Table II) is small, about 1%. In addition, since the temperatures observed in flares do not exceed $3\cdot 10^7$ °K, the transition layer, as follows from calculations, cannot sink into the region where $n_H \geqslant 8\cdot 10^{13}$ cm^{-3}. As a result, the optical (predominantly H_α) emission of the parts of the flare which are heated by the heat flux cannot exceed 10^7 erg · cm^{-2} · sec^{-1}. This is clearly not sufficient to explain the H_α emission in the kernels of large flares, where the observed energy flux of H_α emission from unit surface is an order of magnitude higher.[54] In addition, in the case of slow heating $p = \text{const}$, the boundary energy flux is small, and for a flare power up to 10^{29} erg/sec presupposes that its area is not less than 10^{20} cm^{-2}. Thus, the heating regime $p = \text{const}$ is not relevant to the flare kernels during the explosive phase but is realized during the third, hot phase of the flare, when there is prolonged release of energy over the whole area of the flare.

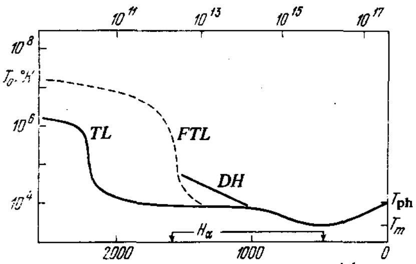

FIG. 5. Height distribution of the temperature in the quiet chromosphere and during a flare. *TL* is the transition layer, T_m is the temperature minimum, T_{ph} is the temperature of the photosphere. The dashed curve shows the flare temperature distribution. *FTL* is the flare transition layer; *DH* is the low-temperature region in the case of direct heating by energetic particles.

This conclusion is also supported by a comparison of the characteristic times. The lifetime of the bright compact (1″) points in the flare kernels is about 5 sec (as an example, consider the impulsive flare on August 2, 1972 at 1838 UT[54]); it is shorter than the characteristic gas-dynamic time in the chromosphere, i.e., the inequality (2.3) holds, and the case $n = \text{const}$ of rapid heating can be realized. In contrast, the hot phase of the flares usually lasts tens of minutes or even hours. In this case the inequality (2.2) is obviously satisfied, and there is time for the gas pressure to be equalized during the heating process.

Let us consider the case $n = \text{const}$ of rapid heating. Here, as Table II shows, temperatures above $2\cdot 10^7$ °K can be achieved only for excessively large boundary energy fluxes. However, most frequently, the observed temperatures $(1-2)\cdot 10^7$ °K require energy fluxes that do not contradict the observations of the hard x-ray emission (see Chap. 3). At the same time, as Table II shows, the predicted flux of H_α emission from unit surface of the flare kernel in the regime of rapid thermal conduction heating does not exceed $3\cdot 10^7$ erg · cm^{-2} · sec^{-1}. Thus, in the case $n = \text{const}$ as well the thermal conduction mechanism of heating of the low-temperature (optical) region of the flare in the chromosphere is not effective for explaining the optical emission of the flare kernels (especially if one takes into account the optical continuum observed in large flares), and one must invoke other nonthermal mechanisms for heating the solar atmosphere. Note also that even in the case of processes as fast ($\lesssim$ 5 sec) as those associated with the bright points in the kernels the actual gas-dynamic picture may differ from the limiting regime $n = \text{const}$ considered above. Obviously this difference tends to equalize the pressure and to reduce the boundary energy flux needed for heating to the observed boundary temperatures.

E. Thermal x-ray emission. Hot phase of the flare and thermal waves

The emission of the high-temperature flare plasma, mainly thermal x rays, is usually described in terms of effective temperatures and the emission measure.

The former characterizes the slope of the spectrum in the given spectral band and the latter the magnitude of the flux in the same band. The time behavior of the temperature and the emission measure and also the variation with time of the temperature dependence of the emission measure for the thermal x-ray bursts associated with solar flares have now been well studied[51,52] (see also[48–50,53]). In particular, it is known that in the overwhelming majority of thermal x-ray bursts the temperature rapidly increases at the start of the burst and then slowly decreases. The maximum of the emission measure is reached much later than the maximum of the temperature. Thus, for a certain time the growth of the emission measure is accompanied by a fall in the temperature. This recalls the natural process of cooling of a hot region through thermal conduction heating of a neighboring cold region, i.e., the propagation of a thermal wave from the hot to the cold region. Since it is however known from observations that the thermal energy of the complete hot plasma increases during this stage, one must assume, in addition to the original heating, the presence of a thermal source that is operative during the complete x-ray burst. During the hot phase, such a heat source could be the turbulent heating of the plasma in the region of breaking of the current sheet. Thus, the heating of new cold matter during the prolonged liberation of thermal energy because of the rejoining of the magnetic lines of force after the breaking of the sheet can evidently be the mechanism responsible for the observed growth of the emission measure of the soft x rays.

In[55], Moore and Datlowe calculated the characteristic heating and cooling times of a high-temperature plasma for a number of small (importance $\leqslant 1$) solar flares on the basis of the observed temperatures and emission measures at the maximum of the thermal x-ray flux, the duration of this maximum, and the characteristic linear dimension of the flare. It was found that the empirical values of the characteristic times for different flares in the framework of similarity theory agree with the assumption that the rejoining of the magnetic lines of force is the heat source. Comparison of the characteristic times showed that the heat conduction cooling of the high-temperature plasma predominates over radiative cooling and approximately equalizes the heating of the plasma by the magnetic rejoining.

With the aim of explaining the observed behavior of the temperature and the emission measure of the thermal x rays, some authors[53,56,57] solved numerically the problem of the propagation from a heat source of a thermal wave with emission losses through a homogeneous corona; namely, equations (1.11) and (1.12) under the assumption that $T_e = T_i$, $n = \text{const}$, and $v = 0$. In such an approach there are two shortcomings. First, the thermal wave creates in the gas large temperature and pressure gradients, which unavoidably lead to rapid gas-dynamic motions. These can give rise to powerful shock waves, which considerably change the complete picture of the phenomenon. Redistribution of matter must be taken into account at the least as the final result of the gas-dynamic motions, these tending to equalize the gas pressure.[40,41,58] Second, as is well known, heating of only the coronal gas is not adequate to explain the observed emission measure in the x-ray range; it is necessary to heat the chromosphere or dense and massive cold formations in the corona, whose emission measure is comparable with the corona's. Here again one needs gas-dynamic motions, which carry matter into the hot corona of the flare.

F. Other sources of heating of the high-temperature flare plasma

Only two heat sources of the hot flare plasma can be important[34]: heat liberated in the neutral current sheet as a result of quasistationary dissipation of the magnetic field or the breaking of the current sheet in the presence of anomalous resistance (thermal or soft phase of the flare) and energetic particles accelerated at the time when the sheet breaks (nonthermal or hard phase). The thermal heating source has been mainly assumed above. It is well known however that in the nonthermal process the greatest power of energy release is achieved and a total amount of energy sufficient to ensure all the observed manifestations of the flare is released.[59–64] Therefore, accelerated particles can heat the hot flare plasma during the explosive phase to anomalously high temperatures. This is particularly true of large flares. At the same time, it must be borne in mind that in small (importance $\leqslant 1$) flares there may not be a nonthermal component at all[51] or it may be so weak that the nonthermal electrons are not the main source of heating of the high-temperature region of the flare.[65]

With regard to the other mechanisms for heating the solar atmosphere, for example, dissipation of shock and magnetohydrodynamic waves, they cannot make a significant contribution to the heating of the high-temperature flare plasma.

G. X-ray and ultraviolet emission of the high-temperature region and its geometry

The hot flare plasma emits a large amount of energy in a wide range of wavelengths: basically in the soft x-ray range and the ultraviolet, both in the continuum and lines. In principle, this enables one to obtain exhaustive information about the high-temperature region of the flare from the numerous rocket and satellite observations (see, for example,[51,52,66–77a]). As an example, let us consider the continuum x rays of the high-temperature region. Suppose there is only one magnetic tube, which is heated by a stationary heat flux, as was described above. Then, knowing the temperature distribution $T(\xi)$ over the thickness of the matter along an individual magnetic tube, one can readily calculate the spectrum of thermal continuum x-ray emission. We shall call it the *elementary* x-ray spectrum. For a tube with unit cross section[45,78]

$$j(E_x) \simeq 3.9 \cdot 10^{-3} n_\infty A(E_x, T_0) \quad (\mathrm{erg \cdot cm^{-2} \cdot sec^{-1} \cdot keV^{-1}}), \tag{2.5}$$

where E_x is the energy of the x rays in keV,

$$A(E_x, T_0) = \int\limits_{\xi_{\min}}^{\xi(T_0)} T^{-0.5} \frac{T_\infty}{T} \exp\left(-\frac{E_x}{kT}\right) d\xi; \tag{2.6}$$

here we have taken into account only the thermal bremsstrahlung; the dependence $T(\xi)$ is taken from[41] for the case p = const, and the unit for measuring ξ is $1.5 \cdot 10^{17}$ cm^{-2}. In Fig. 6, which shows elementary spectra calculated in accordance with Eqs. (2.5) and (2.6) for different boundary temperatures T_0, it can be seen that these spectra differ from exponential spectra corresponding to T_0 (see the dashed straight line for $T_0 = 3.10^7$ °K) only in the region of the softest x rays: $E_x \lesssim 5$ keV. This difference is small and due to the contribution of the parts of the tube that have a lower temperature.

Observations show that many flares (especially large ones) can have a region with very high temperatures up to $3 \cdot 10^7$ °K (see[50, 51, 67–73]) and probably sometimes up to $5 \cdot 10^7$ °K. The thermal x-ray emission of such hot regions may make an appreciable contribution right up to the energy 30 keV. In addition, such flares have as a rule a source of softer x rays, whose temperature is much lower (from $(2-3) \cdot 10^6$ to 10^7 °K) and emission measure 2–3 orders of magnitude greater,[52, 68, 69] which cannot be explained by one elementary spectrum alone. Therefore, in order to construct a model x-ray spectrum of the flare as a whole, it is necessary to take not less than two tubes: one with a very high boundary temperature but low emission measure and second with lower temperature but extremely large emission measure. A real flare must be regarded as a collection of elementary tubes with different F_0's (or T_0's) and n_∞'s. In this way, one can explain the observed temperature dependence of the emission measure of the x rays.[52] At the same time, only the high-temperature component of the source of thermal x rays is intimately related to the electrons accelerated during the explosive phase. By and large, this picture is confirmed by space observations in the ultraviolet and soft x-ray lines of highly ionized elements,[71, 73–77] and also by the observations of hard x-ray and microwave radio bursts that are simultaneous with optical bursts in flare H_α kernels (see, for example,[54, 79–81]).

Much information about the space and time development of the region of the high-temperature flare plasma was obtained in the GSFC experiment on the satellite OSO-7.[71] Two x-ray (1.74–15.9 Å) and one ultraviolet (120–400 Å) spectrographs obtained data on the high-temperature region of the 1B flare on August 2, 1972 at 1838 UT from the pre-flare state until its end. Emission lines excited at electron temperatures from $5 \cdot 10^4$ to $3 \cdot 10^7$ °K were resolved. The spatial resolution was 20"×20".

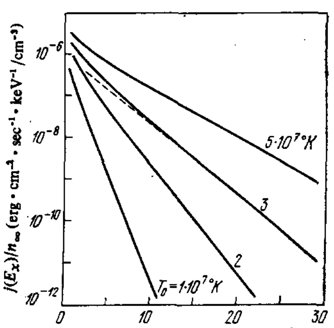

FIG. 6. Energy spectrum of thermal bremsstrahlung x rays of hot plasma heated by a heat flux within a magnetic tube with unit cross sectional area.

At least two arched structures with different properties were observed in the x-ray emission. The first, with a relatively low temperature $2 \cdot 10^6 \lesssim T \lesssim 10^7$ °K, was formed during the explosive phase directly above the H_α flare and formed a system of low arches above the "neutral" line of the magnetic field. Simultaneously, an arch with temperature up to $3 \cdot 10^7$ °K and height up to 35000 km became visible in the line 1.9 Å FeXXV. The bases of this arch were situated above the brightest regions of the H_α emission. The electron temperature within the arch increased from $5 \cdot 10^6$ °K directly above the chromosphere to $3 \cdot 10^7$ °K at the crown of the arch situated above the zero line of the magnetic field, i.e., between the flare ribbons in the projection onto the disk, as the flare was observed. It was shown in[71] that the observed further variations in the localization of the x-ray source were simply the result of the variation of the electron temperature with time. In particular, the high-temperature arch cooled during about 10 min from $3 \cdot 10^7$ to $1 \cdot 10^7$ °K, which, generally speaking, does not contradict the assumption of heat conduction cooling of the hot plasma through the ends of the arch if allowance is made for the uncertainty of the parameters and the simple nature of the expressions used (see[39]).

A similar behavior of the high-temperature region was observed in the two-ribbon flare of June 15, 1973 by means of the NRL ultraviolet (170–630 Å) spectrograph on Skylab[73] with spatial resolution down to 2". These and subsequent observations[74, 75] confirmed the presence of a temperature stratification within individual loops and showed that the hottest plasma, observed in the lines Fe XXIII–XXIV, occupies a small volume at the crowns of the loops. It is apparently here that the primary liberation of energy occurs in the hot phase of the flare. Observations by means of AC/MSFC, the x-ray (6–47 Å) telescope S-056 on Skylab[76, 77] with spatial resolution ~1" showed that the flare energy liberation takes place not in one loop but in an arcade of loops. In addition, the order in which the different x-ray features brightened indicates that a certain excitation moves perpendicularly to the magnetic field of the arcade with a velocity 180–280 km/sec. This picture suggests that the energy source—the current sheet—passes along the crowns of the loops and is gradually displaced into the corona. The decay of the dense plasma in the sheet into individual filaments—loops—is evidently due to an instability of the sheet.

Thus, the spatial and time observations[71, 73–77] in the x-ray and ultraviolet lines agree on the whole with the picture of the high-temperature region of the flare as a collection of elementary tubes with different F_0's (or T_0's) and n_∞'s, which depend on the time; this follows from the analysis of the x-ray continuum.

3. ENERGETIC PARTICLES IN THE ATMOSPHERE OF THE SUN

A. Electrons accelerated in the flare. Thermal and nonthermal x-ray emission

One of the most important processes that takes place in the energy source of the flare—the current sheet—

is the acceleration of charged particles to high energies. For the overwhelming majority of flares that exhibit an explosive phase, the accelerated particles are electrons with an energy greater than about 10 keV (see the reviews[81,82]). Only in very powerful flares are protons accelerated, or at least in significant quantities.[46,83]

The energetic electrons generate bursts of hard (with x-ray energy E_x greater than 10 keV) x-ray emission with a power-law spectrum of the x-ray flux at the Earth:

$$\frac{dI(E_x)}{dE_x} = K_\varphi E_x^{-\varphi}\ (\mathrm{cm^{-2}\cdot sec^{-1}\cdot keV^{-1}}). \tag{3.1}$$

Here and below, E_x is always the energy of the x rays in keV, and the coefficient K_φ is measured in $\mathrm{cm^{-2}\cdot sec^{-1}\cdot keV^{\varphi-1}}$, respectively. These bursts are interpreted as the bremsstrahlung of nonthermal electrons.[84–87]

In addition, giving up the overwhelming part of their energy to the solar atmosphere, the accelerated electrons heat it locally to high temperatures. These temperatures can, as we have already noted, be so high that the thermal x rays of the hot flare plasma are hard. This circumstance makes it difficult to interpret the hard x-ray bursts and the interpretation is, generally speaking, unambiguous in two respects.

First, the thermal x-ray emission of the high-temperature flare plasma masks the lower boundary of the nonthermal x-ray spectrum.[48,88] Therefore, to determine the lower end of the energy spectrum of the accelerated electrons it is necessary to invoke additional arguments and observational data. For example, if one assumes that the energetic electrons are the main source of heating of the high-temperature region, then the energy balance condition in it can give an estimate of the necessary power of the electron beam. If the exponent of the spectrum is known, the total power is uniquely related to the lower end of the energy spectrum of the accelerated electrons. In the framework of such an approach[89] the spectrum of energetic electrons can be recovered only by using observational data on the high-temperature region: the spectra in the ultraviolet and soft x-ray region and their variations in time and distributions in space.

Second, since the primary heating may not be due to electrons, there is an alternative point of view whose essence is that there are no nonthermal electrons at all. This is the so-called thermal interpretation of the hard x-ray bursts[90,91] (see also[92]). In it, a flare is regarded as a purely thermal process, in contrast to a nonthermal conception, in which the hard x-ray bursts are a direct manifestation of the nonthermal phase of the flare. In[93], Kahler categorizes the thermal interpretation as pessimistic since it enables one to calculate only the total amount and rate of conversion of flare energy into heat. In contrast, by developing a theory of hard x-ray bursts as the bremsstrahlung of nonthermal electrons,[60,64] one can obtain information about the acceleration process in the flare. Note that the correct expression for the intensity in the "thick target" model is given in[64] (see Eq. (3.8) below); in[60], a coefficient π has been lost. At the present time, the nonthermal interpretation is predominant since accelerated electrons are manifested not only in the x-ray bursts but also in radio bursts of type III and other types (see, for example,[94,95]) and are also directly detected on satellites in interplanetary space (see, for example, the review[96]).

Below, we shall briefly discuss some of the simplest models of hard x-ray emission that exist in the framework of the nonthermal interpretation. These models are of great interest since, under certain simplifying assumptions,[64,97] they enable one to establish the spectrum of the electrons accelerated in the flare from the spectrum of x rays observed at the Earth. It is also important that these models are limiting cases that must be satisfied by a more complete and adequate theory of hard x-ray bursts.

B. Spectrum of energetic electrons and choice of the target model

The question of the spectrum of the electrons accelerated in a flare in connection with hard solar x-ray bursts was posed by Peterson and Winckler[98] as long ago as 1959. The first traces of hard x-ray bursts,[98] which were interpreted as Coulomb bremsstrahlung of electrons with energy higher than 10 keV, showed, and the subsequent observations confirmed, that the electrons accelerated during the explosive phase of the flare can contain an energy sufficient to explain the observed emission of the flare in all energy ranges.[59–64] Simultaneously, it became clear that the problem of establishing the spectrum of the energetic electrons is neither simple nor unambiguous (see[99–101]). The known uncertainty in establishing the connection between the hard x rays and the electrons generating them appears already in the choice of the target model.

Suppose that the characteristic time τ_c of Coulomb collisions of electrons of the beam with electrons of the plasma is much shorter than the characteristic injection time τ_i of the energetic electrons. Then the injection can be regarded as stationary or continuous, as one says.

Suppose the differential energy spectrum of the flux of injected ($\xi=0$) electrons has a power law in the range of energies between E_1 and E_2:

$$v(E)N(E,0) = K_\gamma E^{-\gamma}\theta(E-E_1)\,\theta(E_2-E)\ (\mathrm{cm^{-2}\cdot sec^{-1}\cdot keV^{-1}}), \tag{3.2a}$$

and accordingly the electron density is

$$N(E,0) = KE^{-\gamma-(1/2)}\,\theta(E-E_1)\,\theta(E_2-E)\ (\mathrm{cm^{-3}\cdot keV^{-1}}). \tag{3.2b}$$

Here, $\theta(x)$ is the theta function: $\theta(x)=0$ for $x<0$ and $\theta(x)=1$ for $x\geqslant 0$. The variable E, measured in keV, is the energy of the electrons, which are assumed nonrelativistic, and the coefficient K_γ is given by

$$K_\gamma = K\sqrt{\frac{2}{m}} \approx 1.87\cdot 10^9 K\ (\mathrm{cm^{-2}\cdot sec^{-1}\cdot keV^{\gamma-1}}), \tag{3.2c}$$

where m is the electron mass in keV/c^2, c is the veloc-

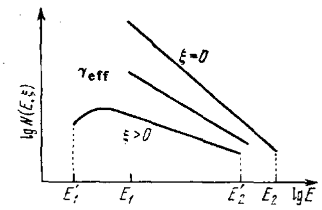

FIG. 7. Energy spectrum of nonthermal electrons. $\xi = 0$ is the spectrum of the accelerated electrons, or the injection spectrum; $\xi > 0$ is the spectrum of electrons that have passed through a thickness ξ of matter; γ_{eff} is the effective (total) spectrum of the energetic electrons in the emission source.

ity of light in cm/sec, and the coefficient K is measured in $\mathrm{cm}^{-3}\cdot\mathrm{keV}^{\gamma-(1/2)}$.

After the energetic electrons have traversed a matter thickness ξ cm^{-2} in the ionized plasma, the spectrum is shifted as a result of Coulomb losses to lower energies and it becomes harder[64]:

$$N(E, \xi) = K\sqrt{E}\,(E^2 + E_0^2)^{-(\gamma+1)/2}\,\theta(E - E_1')\,\theta(E_2' - E)\ (\mathrm{cm}^{-3}\cdot\mathrm{keV}^{-1}); \tag{3.3}$$

where

$$E_0 = \sqrt{2a\xi} \tag{3.4}$$

is the minimal initial energy of electrons capable of traversing the thickness ξ, $a \simeq 3\cdot 10^{-18}$ cm^2 is the coefficient which characterizes the Coulomb losses:

$$\frac{dE}{d\xi} \approx -\frac{a}{E}, \tag{3.5}$$

$E_{1(2)} = \mathrm{Re}\sqrt{E_{1(2)}^2 - E_0^2}$ are new limiting energies of the electron spectrum (see the schematic Fig. 7).

There are two opposite limiting cases that attract attention.

1) *Thin target*. The energetic electrons pass through a thickness of matter that is so small as to allow one to ignore the change of their spectrum in the source of the bremsstrahlung x-ray emission. In this case, the differential spectrum of the x-ray flux at the Earth is given by

$$\begin{aligned}\frac{dI(E_x)}{dE_x} &= \frac{1}{4\pi R^2}\int_V dV \int_{E_x}^{\infty} dE\,\frac{d\sigma}{dE_x}\,nvN(E, \xi)\\ &= \frac{1}{4\pi R^2}\int_S dS \int_0^{s_t} n(s)\,ds \int_{E_x}^{\infty} dE\,\frac{d\sigma}{dE_x}\,vN(E, 0)\\ &= \frac{1}{4\pi R^2}\left(\frac{8r_0^2}{3}\,\alpha z^2 mc^2\right)\int_S dS\,\xi_t K_\gamma\,\frac{B(\gamma, 1/2)}{\gamma}\,E_x^{-(\gamma+1)}\\ &= 1.74\cdot 10^4 \int_S \frac{dS}{S^*}\,\frac{\xi_t}{\xi^*}\,\frac{K_\gamma}{K_\gamma^*}\,\frac{B(\gamma, 1/2)}{\gamma}\,E_x^{-(\gamma+1)}\ (\mathrm{cm}^{-2}\cdot\mathrm{sec}^{-1}\cdot\mathrm{keV}^{-1}),\end{aligned} \tag{3.6}$$

where R is the distance from the flare to the point of observation and in (3.6) we have taken $R = 1.5\cdot 10^{13}$ cm. The integration over the volume V of the target is made under the assumption that the curvature of the lines of force can be ignored and one can set $dV = dSds$, where S is the cross sectional area of the electron beam and $S^* = 10^{18}$ cm^2 is the characteristic area of the flare taken as unit of measurement for S. The thickness of the target $\xi_t = \int_0^s n(s)\,ds$ is measured in units of $\xi^* = 10^{18}$ cm^{-2}. The coefficient K_γ is determined by Eq. (3.2c), and the characteristic value is $K_\gamma^* = 6.24\times 10^{19}$ $\mathrm{cm}^{-2}\cdot\mathrm{sec}^{-1}\cdot\mathrm{keV}^{\gamma-1}$. The differential bremsstrahlung cross section $d\sigma/dE_x$ is taken in the Bethe–Heitler approximation, r_0 is the classical electron radius, α is the fine structure constant, and z is the effective charge of the ions. $B(x, y)$ is the beta function: $B(\gamma, 1/2) = 16/15$, $32/35$, 0.812 and 0.738 for $\gamma = 3$, 4, 5, and 6, respectively.

As can be seen from (3.6), in the approximation of a thin target, the exponent of the differential spectrum of the x-ray flux at the Earth is greater by unity than the exponent of the differential spectrum of the flux of nonrelativistic electrons on the Sun (see[62,84]), i.e.,

$$\varphi = \gamma + 1. \tag{3.6a}$$

2) *Thick target*. All electrons lose their energy in the source of the hard x rays. Therefore, at all times in the source there are energetic electrons with not only the injection spectrum (3.2) but also with all the harder spectra (3.3) with ξ values from 0 to ∞. This means that in the main energy range $E_1 \lesssim E \lesssim E_2$ the effective (total) spectrum of electrons in the source of hard x rays is harder by two units[60,64]:

$$\gamma_{eff} = \gamma - 2, \tag{3.7}$$

and the differential spectrum of the x-ray flux at the Earth is[64]:

$$\begin{aligned}\frac{dI(E_x)}{dE_x} &= \frac{1}{4\pi R^2}\int_S dS \int_{E_x}^{\infty} dE\,\frac{d\sigma}{dE_x}\int_0^{\infty} d\xi\,vN(E, \xi)\\ &= \frac{1}{4\pi R^2}\left(\frac{8r_0^2}{3}\,\alpha z^2 mc^2\right)\frac{1}{a}\int_S dS K_\gamma\,\frac{B(\gamma-2;\ 1/2)}{(\gamma-1)(\gamma-2)}\,E_x^{-(\gamma-1)}\\ &= 5.8\cdot 10^3 \int_S \frac{dS}{S^*}\,\frac{K_\gamma}{K_\gamma^*}\,\frac{B(\gamma-2,\ 1/2)}{(\gamma-1)(\gamma-2)}\,E_x^{-(\gamma-1)}\ (\mathrm{cm}^{-2}\cdot\mathrm{sec}^{-1}\cdot\mathrm{keV})\end{aligned} \tag{3.8a}$$

or

$$\begin{aligned}\frac{dI(E_x)}{dE_x} &= \frac{1}{4\pi R^2}\left(\frac{8r_0^2}{3}\,\alpha z^2 mc^2\right)\frac{1}{a}\,\frac{B(\gamma-2;\ 1/2)}{\gamma-1}\,E_1^{\gamma-2}E_x^{-(\gamma-1)}\int_S dS\,F_0(E > E_1)\\ &\simeq 5.8\cdot 10^3\,\frac{B(\gamma-2;\ 1/2)}{\gamma-1}\,E_1^{\gamma-2}E_x^{-(\gamma-1)}\int_S \frac{dS}{S^*}\,\frac{F_0(E > E_1)}{F^*}\ (\mathrm{cm}^{-2}\cdot\mathrm{sec}^{-1}\cdot\mathrm{keV}^{-1})\end{aligned} \tag{3.8b}$$

$B(\gamma - 2;\ 1/2) = 2$, $4/3$, $16/15$, and $32/35$ for $\gamma = 3$, 4, 5, and 6, respectively.

It can be seen that the exponent of the x-ray spectrum is

$$\varphi = \gamma_{eff} - 1 = \gamma - 1. \tag{3.8c}$$

In deriving (3.8), we have assumed that the upper end E_2 of the electron spectrum is fairly high: $E_2 = \infty$.

Accordingly, in Eq. (3.8b)

$$F_0(E > E_1) = 1.602\cdot 10^{-9}\,K_\gamma E_1^{2-\gamma}/(\gamma - 2)\ (\mathrm{erg}\cdot\mathrm{cm}^{-2}\cdot\mathrm{sec}^{-1}), \tag{3.9}$$

is the boundary energy flux of electrons with energy $E > E_1$. The characteristic flux is $F^* = 10^{10}$ $\mathrm{erg}\cdot\mathrm{cm}^{-2}\cdot\mathrm{sec}^{-1}$, corresponding to the above characteristic value $K_\gamma^* = 6.24\cdot 10^{19}$ $\mathrm{cm}^{-2}\cdot\mathrm{sec}^{-1}\cdot\mathrm{keV}^{\gamma-1}$ for $E_1^* = 10$ keV and $\gamma^* = 3$.

3) *Intermediate cases.* All the intermediate cases must be characterized by a certain thickness of the target or an effective time τ_e of emergence of the energetic electrons from the emitting region. In terms of the latter, for continuous ejection the case of thin target corresponds to this relation between the characteristic times:

$$\tau_e \ll \tau_c \ll \tau_i, \tag{3.10}$$

while for a thick target

$$\tau_c \ll \tau_e \ll \tau_i \tag{3.11}$$

(see the reviews[81,101]). Nothing in fact is known about τ_e (in particular, about its dependence on the electron energy) except that only an insignificant fraction of the electrons accelerated in the flare reach interplanetary space. Generally speaking, this favors the thick target model, though it does not contradict more complicated combined models with a thick target in conjunction with a magnetic trap, etc. (see below). The construction of a realistic and rigorous theory of the escape of the accelerated particles from the flare region is one of the most important unresolved problems of solar physics. Some investigations concerning the diffusion escape of energetic particles from closed magnetic structures in the region of the flare can be found, for example, in[102]. Takakura[103] has shown that plasma turbulence effects can play an important role in the dynamics of the escape of electrons with energy higher than 100 keV. However, at lower energies these effects are apparently unimportant.

C. Thick target and more complicated models

To estimate the total energy and number of energetic electrons from the observed intensity of the hard x rays, Lin and Hudson[62] proposed an approximate method based on calculating the average value of the ratio of the bremsstrahlung losses to the collision and ionization losses. A developed theory of hard x-ray bursts in the thick target model was constructed by Brown[60] and Syrovatskiĭ and Shmeleva.[64] In particular, the latter[64] obtained the solution (3.3) of the transport equation of energetic electrons with power-law spectrum in the presence of Coulomb losses in a fully ionized plasma. They showed that the effective (total) spectrum of emitting electrons is appreciably harder than the spectrum of the accelerated electrons. They obtained expressions that enable one to calculate the slope of the spectrum of the energetic electrons, their total energy, and their number from the observed spectrum of the nonthermal x-ray emission of the flare. Namely, if the differential spectrum of the x-ray flux (3.1) is known, i.e., the parameters K_φ and φ are known, then the power introduced by the electrons with energy $E > E_1$ is determined by (see (3.8))

$$\mathcal{F}(E > E_1) \equiv \int\limits_S F(E > E_1)\, dS = 4\pi R^2 \left(\frac{8r_0^2}{3}\alpha z^2 mc^2\right)^{-1} a\, \frac{(\gamma-1)}{B(\gamma-2;\ 1/2)} \times K_\varphi E_1^{2-\gamma} = 1{,}72\cdot 10^{25}\, \frac{(\gamma-1)}{B(\gamma-2;\ 1/2)}\, K_\varphi E^{2-\gamma}\ (\text{erg}\cdot\text{sec}^{-1})\,; \tag{3.12}$$

where $\gamma = \varphi + 1$, E_1 is measured in keV, K_φ in $\text{cm}^{-2}\cdot\text{sec}^{-1}\cdot\text{keV}^{\varphi-1}$, and the beta function $B(\gamma-2;\ 1/2) = 2$, 4/3, 16/15, and 32/35 for $\gamma = 3$, 4, 5, and 6, respectively.

As an example let us consider the impulsive flare on August 2, 1972 at 1838 UT. According to the UCSD x-ray telescope on OSO-7 the x-ray flux at the Earth averaged over 10.2 sec at the maximum of the hard x-ray (20–30 keV) burst at 1839:52 UT has a power-law spectrum with $K_\varphi \approx 10^7\ \text{cm}^{-2}\cdot\text{sec}^{-1}\cdot\text{keV}^{\varphi-1}$ and $\varphi = 3.7$ (see Fig. 4 in[104]). Using (3.12), we find the power of the energetic electrons on the Sun $\mathcal{F}(E > 10\ \text{keV}) \approx 6\cdot 10^{29}\ \text{erg}\cdot\text{sec}^{-1}$ and $\mathcal{F}(E > 20\ \text{keV}) \simeq 7.6\cdot 10^{28}\ \text{erg}\cdot\text{sec}^{-1}$ for $E_1 = 10$ and 20 keV, respectively. If one takes the area $S_2 \simeq 5\cdot 10^{17}\ \text{cm}^2$ of the flare kernel at this time, then these values of the power correspond to boundary energy fluxes $F_0(E > 10\ \text{keV}) \simeq 10^{12}\ \text{erg}\cdot\text{cm}^{-2}\cdot\text{sec}^{-1}$ and $F_0(E > 20\ \text{keV}) \simeq 1.5\cdot 10^{11}\ \text{erg}\cdot\text{cm}^{-2}\cdot\text{sec}^{-1}$.

If the total flux of x rays at the Earth in a certain energy range $E_{x1} \leqslant E_x \leqslant E_{x2}$ is known, then the power of electrons with energy $E > E_1$ and their total number are determined by

$$\mathcal{F}(E > E_1) = 4\pi R^2 \left(\frac{8r_0^2}{3}\alpha z^2 mc^2\right)^{-1} a\, \frac{(\gamma-1)(\gamma-2)}{B(\gamma-2;\ 1/2)} \times \left[1 - \left(\frac{E_{x1}}{E_{x2}}\right)^{\gamma-2}\right]^{-1} \left(\frac{E_{x1}}{E_1}\right)^{\gamma-2} I(E_{x1} < E_x < E_{x2}) \simeq 1.63\cdot 10^{25}\, \frac{(\gamma-2)(\gamma-1)}{B(\gamma-2;\ 1/2)}\, \frac{I(E_{x1} < E_x < E_{x2})}{1-(E_{x1}/E_{x2})^{\gamma-2}} \left(\frac{E_{x1}}{E_1}\right)^{\gamma-2} (\text{erg}\cdot\text{sec}^{-1}), \tag{3.13}$$

$$\Phi(E > E_1) \equiv \int\limits_S dS \int dE\, vN(E,\ 0) = 1.02\cdot 10^{34}\, \frac{(\gamma-2)^2}{E_1 B(\gamma-2;\ 1/2)}\, \frac{I(E_{x1} < E_x < E_{x2})}{1-(E_{x1}/E_{x2})^{\gamma-2}} \left(\frac{E_{x1}}{E_1}\right)^{\gamma-2} (\text{sec}^{-1})\,. \tag{3.14}$$

In contrast to the thin target model, the thick target model does not require assumptions about the plasma concentration in the emitting region (or rather about the target thickness ξ_t; see (3.6)); it is only necessary that the conditions (3.11) be satisfied. In this respect, the thick target model requires for the description of a hard x-ray burst the minimal number of parameters, namely, three (see (3.12))—the instantaneous energy flux of the electrons with energy above a certain value E_1, i.e., $F_0 = F_0(E > E_1)$, the value of this limiting energy E_1, and the instantaneous slope exponent of the spectrum. Any other models require specification of additional parameters, for example, the plasma concentration in an electron trap or the escape time in the thin target model, i.e., $s_t/v(E)$ in (3.6). It is obvious that from the point of energy a thick target is the most advantageous for two reasons. First, in all the remaining cases only some of the accelerated electrons give up their energy on bremsstrahlung and heating of the target, while the remaining electrons escape with hardly any loss into interplanetary space. Second, in the interpretation of a hard x-ray burst with spectral exponent φ the thick target model gives the softest (steepest) spectrum of energetic electrons, which enables one to accumulate a greater part of the electron energy near the lower boundary. Unfortunately, it is the lower end of the electron energy spectrum that is not exactly determined since the lower end of the nonthermal x-ray spectrum is unknown.

It is easy to imagine a thick target model with impulsive injection. By this we mean the case when all the energetic electrons "perish" in the target (there is no escape) but the injection time τ_i is much shorter than the Coulomb collision time τ_c (see[101]):

$$\tau_i \ll \tau_c \ll \tau_e. \tag{3.15}$$

A conceivable example of such a situation could be a magnetic trap filled with low-density plasma into which energetic electrons are injected. Suppose that seepage of the electrons from the trap can be ignored and that the energy losses of the electrons are determined solely by Coulomb collisions. In pure form, such a situation is clearly never realized in flares, but from the point of view of fundamentals it is interesting in that the characteristic time of damping of the hard x-ray burst is here determined by the Coulomb loss time

$$\tau_c \simeq 3.3 \cdot 10^8 n^{-1} E^{3/2} \text{(sec)}, \tag{3.16}$$

where E is the energy of the electrons in keV.

As a rule, the observed damping time does not follow the law $E^{3/2}$, which indicates that either the damping of the x-ray burst is determined by the escape of the energetic electrons or that the electrons perish in the thick target at high plasma concentrations, i.e., the conditions (3.11) are satisfied. In the latter case, the time profile of the x-ray burst is determined by the source of the accelerated particles.

Observations by means of the Utrecht solar hard x-ray spectrometer on the satellite ESRO TD-1A with time resolution 1.2 sec in the region 24–90 keV and 4.8 sec at higher energies showed that frequently the x-ray bursts consist of numerous short-lived spikes, or "elementary flare bursts," with rise and fall times of the order of few seconds.[105,106] Characteristically, the fall times (sometimes only 1–2 sec) were practically the same in all energy channels. This indicates a very high plasma concentration in the region of the thick target.[105,106] If the target is the chromosphere, then obviously the lifetime of an energetic electron is comparable with the time of passage through several scale heights and is much shorter than the observed decay time of an elementary burst. In this case the time dependence of the burst will be determined by the source of the accelerated electrons.

To explain the quasiperiodic time profile of the large x-ray event associated with the 3B flare on August 4, 1972, Brown and Hoyng[107] (see also[108,109]) proposed a model of a vibrating electron trap. In this model, the repeated bursts of hard x rays are explained by betatron modulation of electrons accelerated previously by Alfvén oscillations of the magnetic trap. For an appropriate choice of the trap parameters, the model can be reconciled with the observations of the hard x-ray bursts from flares behind the limb.[110,111] However, these observations also do not contradict the ordinary thick target model if it is assumed that the source of energetic electrons is at an appreciable height (~10 000 km) in the corona and that the plasma density near the source is increased by, for example, a preliminary heating and "evaporation" of the upper chromosphere.[112] In addition, the model of a vibrating trap is hard to reconcile with the observational fact emphasized by de Feiter[81,101,113] that individual pulses in a complicated x-ray burst correspond to the appearance of bright optical (H_α, λ 3835) kernels at different points of the chromosphere. Moreover, according to observations by means of the AC/MSFC x-ray telescope S-056 on Skylab,[76,77] the flare energy liberation does not occur instantaneously and in one region (one trap) but successively in different magnetic loops that form an arcade above the zero line of the photospheric magnetic field.

D. Heating of the chromosphere by energetic electrons. Thermal and penetrating flares

Heating of the chromosphere by particles accelerated in a flare (electrons, protons, and nuclei of heavier elements) has been assumed and discussed by many authors[64,114–116]; for example, in connection with white-light flares.[117,118] As we have already noted, energetic electrons have a number of advantages as the flare heating agent. In contrast to protons, they are accelerated in almost all flares: in all large ones and about 2/3 of the smallest (importance ≤ 1),[65,111] and even in small flares the energy of the accelerated electrons in the region 5–100 keV is comparable with the total flare energy.[119]

For electrons accelerated in a flare with the injection spectrum (3.2) the energy averaged over the spectrum is

$$\overline{E} = \frac{2\gamma-1}{2\gamma-3} E_1 = \left(\frac{5}{3}, \frac{7}{5}, \frac{9}{7}, \frac{11}{9}\right) E_1 \tag{3.17}$$

for $\gamma = 3$, 4, 5, and 6, respectively, i.e., it is always near the lower limit E_1 of the spectrum. The main energy of the electrons resides in the low-energy part of the spectrum. This energy is absorbed in a thin layer, creates a high-temperature region, and is transformed into a heat flux. Therefore, in both the soft and the hard phase of the flare the temperature structure of the flare is determined primarily by heat conduction. This enables one to explain the high-temperature part of the flare, which is responsible for the thermal x rays, and the transition region of the flare, which emits in the optical and ultraviolet ranges. However, only an insignificant part (less than 1%) of the original heat flux (see column five of Table II) penetrates to the low-temperature part of the flare, where we place the region of temperatures $T < 2 \cdot 10^4$ °K, in which the hydrogen lines are basically formed.

However, for a sufficiently hard spectrum an appreciable number of particles (with high initial energies) can penetrate below the transition layer and thus contribute to the flux of energy supplied to the low-temperature region of the flare. Shmeleva and Syrovatskiĭ[41] ignored this contribution. In contrast, Brown[116] determined the temperature structure of this region, taking into account only heating by particles and ignoring heat conduction. We emphasize here that the direct heating by particles can again become important at great depths only as a result of a rapid decrease of the thermal conductivity with the temperature. However, the rapid decrease of the electron thermal conductivity at $T \sim 10^4$ °K is partly compensated by the thermal conductivity of the neutrals $\varkappa_H$, which was not taken into account by Brown. [120]

One can readily find the conditions under which the decisive factor is direct heating of the low-temperature region by energetic electrons and not by heat fluxes. It is obvious that the harder is the electron spectrum the greater the fraction of their energy flux that penetrates into the optical region of the flare. It is therefore simply necessary to compare this part of the flux for different exponents of the spectrum with the corresponding heat flux that penetrates below the transition layer.

We shall assume that in both the compared situations the heating is stationary and leads to temperature and density distributions corresponding to equality of the pressure in the whole of the flare region, i.e., $p = \text{const}$. It is obvious that this is a restricted approach, especially in view of the increasing number of observations which show that the injection of the electrons during the explosive phase and therefore the heating do not have a continuous but an impulsive nature in spatially separated regions (see, for example, [54,80,121–124]). Bearing this circumstance in mind, we shall, following[41], give the same results of calculations corresponding to the case when the pressure in the heated region does not have time to be equalized in the case $n = \text{const}$. Of course, this is in no way a substitute for consistent treatment of nonstationary high-temperature gas dynamic phenomena. Here we only emphasize the circumstance that in the case of rapid heating the approximation $n = \text{const}$ may be more adequate for describing the real distributions of the temperature and density than the approximation $p = \text{const}$. This applies particularly to the case of heating of the low-temperature flare region by particles, [116] since the characteristic time of the observed changes in the hard x ray, H_α, and microwave emissions is frequently of the order of one to several seconds. [54,80,105,106,123,125]

Thus, we consider the heating of the flare region by a beam of nonrelativistic electrons with the power-law spectrum (3.2). The energy flux of the electrons corresponding to this spectrum at the depth of the chromosphere where the matter thickness is ξ is

$$F(\xi) = \int_{E_1'}^{E_2'} Ev N(E, \xi)\, dE \ (\text{erg} \cdot \text{cm}^{-2} \cdot \text{sec}^{-1}) . \tag{3.18}$$

In particular, the energy flux of the electrons at the boundary of the heated region, i.e., at $\xi = 0$, is

$$F(0) = \int_{E_1}^{E_2} Ev N(E, 0)\, dE = K \sqrt{\frac{2}{m}}\, \frac{E_1^{2-\gamma} - E_2^{2-\gamma}}{\gamma - 2} \tag{3.19}$$

for $\gamma > 2$. For integral values of γ the ratio $F(\xi)/F(0)$ was calculated, for example, in[126].

As Petrosyan[127] has shown, the dip observed around ~100 keV in the hard x-ray spectrum may be a consequence of the relativistic directionality of the bremsstrahlung of energetic electrons. Therefore, there are as yet no reliable grounds for cutting off the electron spectrum at energies $\simeq 100$ keV. Below, we consider the case $E_2 = \infty$. We mention here that this last assumption is also made by Brown, [116] but on the basis of the conjecture that electrons with energy above 100 keV do not play a role in the heating of an optical flare. Brown assumes a hydrogen concentration $n_H < 7 \cdot 10^{13}$ cm^{-3} (i.e., $\xi < 10^{21}$ cm^{-2}) in the region of the flare. In fact, however, as Švestka[46] has shown, in flares with $n_e \simeq 3 \cdot 10^{13}$ cm^{-3} and real ionization of hydrogen (see Table I in[46] and the literature quoted there) one can expect a hydrogen concentration n_H from $5 \cdot 10^{13}$ to $2 \cdot 10^{15}$ cm^{-2} in the low-temperature region. At such concentrations, heating of the low-temperature region can be achieved only by electrons from the high-energy region $E \gtrsim 80$ keV of the spectrum.

In the case when the upper limit of the spectrum is infinite, one can use the simpler expression of[126] for the energy flux of the electron beam, namely,

$$\frac{F(\xi)}{F(0)} = \frac{\gamma - 2}{2} B\left(\frac{3}{2}, \frac{\gamma - 2}{2}\right)\left(\frac{E_1}{E_0}\right)^{\gamma - 2} \tag{3.20}$$

where $B/2 = 0.785$, 0.333, 0.196, and 0.137 for $\gamma = 2$, 4, 5, and 6, respectively.

Table II contains the values of the ratio $F(\xi)/F(0)$ calculated in accordance with (3.20) for $E_1 = 10$ keV, $\gamma = 3$–6, and values of ξ cm^{-2} corresponding to a thickness of matter heated by a thermal flux equal in magnitude to $F(0)$. The minimal initial energy E_0 of electrons capable of passing through this thickness ξ of matter is determined by Eq. (3.4) and given in the last column of Table II.

We consider separately two limiting cases: 1) slow heating with $p = \text{const}$, 2) rapid heating with $n = \text{const}$.

1) For the case $p = \text{const}$ in Table II the broken line separates the region of parameters of the model (boundary temperature T_0 and exponent γ of the energy spectrum) in which the contribution of the heat flux to the heating of the low-temperature flare region is certainly greater than the contribution of the nonthermal electrons. In reality, the latter may be even smaller since Eqs. (3.5) and (3.20) do not take into account electron scattering in Coulomb collisions. Consistent allowance for the energy loss of the electron beam obviously requires study of the diffusion of the beam with respect to the angles in the presence of a strong magnetic field.

Brown[128] has attempted an approximate solution of this problem. It follows from his results that the energy flux of the particles decreases with depth much faster than given by Eq. (3.20). Therefore, the estimates given here of the energy loss of the electron beam must be regarded as the minimal values. In addition, the comparison presupposes that at the boundary of the region, energy is supplied only in the form of accelerated particles and that it is rapidly transformed into a heat flux (it is assumed that $F_c(0) \simeq F(0)$. The role of the particles in heating the low-temperature region will be even less if besides the accelerated particles there is already an appreciable heat flux at the boundary $\xi = 0$ of the region. That such a situation is possible is indicated by flares that exhibit no nonthermal effects at all.[46]

Returning to Table II, we note that for the class 1B flares considered by Lin and Hudson[62] and Syrovatskiĭ and Shmeleva[64] the observed exponents φ of the differential spectrum of the x-ray flux at the maximum of the nonthermal x-ray burst (when the spectrum is at its hardest) lie in the interval from 4.4 to 5.

In the thick target model,[60,64] this value corresponds to exponents $\gamma = \varphi + 1 \approx 5.4$–6 of the energy spectrum of the electron flux. For flares with an electron spectrum as soft as this, the main source of heating of the low-temperature region is here definitely a heat flux and not electrons. On the other hand, for large flares with hard spectrum (possibly for white-light flares) one can expect in accordance with Table II the heating of the low-temperature flare region to be determined by energetic electrons.

Finally, as is clear from Table II, for "thermal" flares the energy flux that reaches the low-temperature part of the flare is less than 1% of the total energy flux in the flare. Thus, *thermal* flares must be mainly x-ray and ultraviolet flares. The contribution of the low-temperature region to the total emission of the flare can be significant only in the case of heating by energetic particles with sufficiently hard spectrum and in the case of a low boundary temperature of the hot region. Below, we shall refer to these flares as *penetrating,* because in them the heating is realized directly by accelerated particles that penetrate to the low-temperature region of the flare. From the point of view of the x-ray emission, thermal flares must be characterized by a soft spectrum of the nonthermal hard x rays (or absence of the latter) and a high temperature of the soft thermal x rays. Conversely, for a hard spectrum of the nonthermal x rays we must have penetrating optical flares in the form of bright flare kernels that arise simultaneously with the hard x-ray bursts and pulses of the microwave radio bursts. Usually, soft nonthermal spectra are more characteristic of small flares and hard spectra of large ones. Therefore, in accordance with Table II we must expect that up to 10% (about 10^8 erg $\cdot$ cm^{-2} $\cdot$ sec^{-1}) of the total energy flux can penetrate to the optical region of large flares. As a whole, this picture does not contradict the observations of large flares with characteristic times not shorter than 15–20 sec in the hard x-ray emission (see, for example,[54]).

2) A regime of *rapid heating* n = const or one near to it is apparently realized in the short-lived bright points within the flare kernels during the explosive phase of impulsive flares. In this regime, as Table II shows, the energetic particles for all γ and T_0 carry much more energy below the flare transition region than the heat flux. Therefore, the temperature distribution may be very different from the one considered in[40,41]; namely, a quasiequilibrium distribution temperature may be established (in a time shorter than the characteristic gas-dynamic and characteristic heat conduction times) that is determined by the balance of heating by the energetic electrons (1.4) and radiative cooling (1.5):

$$P(\xi) + \mathcal{F}_\infty(T_\infty, n_\infty)\frac{1}{n} = n_e L(T) \tag{3.21}$$

(cf. Eq. (2.1)). This situation will be discussed in Sec. C of Chap. 4.

E. Heating by energetic protons. White-light—flares protons or electrons?

Protons accelerated in the flare do not give rise to bremsstrahlung x rays. We obtain information about them from interplanetary observations (for example,[129,130]) and from observations of solar gamma rays.[131–134] Relatively complete gamma observations were made only for the flares on August 4 and 7, 1972 and they showed that the nuclear reactions leading to the gamma emission began simultaneously with the hard x-ray emission and continued for not less than 10 min. The ratios of the gamma lines at, for example, 2.23 and 4.43 MeV enable one to estimate the slope of the spectrum of the accelerated protons under certain assumptions about the He^3 abundance in the photosphere. Ramaty and Lingenfelter[135] calculated lines for power-law and exponential spectra of the accelerated particles (mainly protons and α particles) and showed that in the interval 10–100 MeV the differential spectrum of the particles satisfies a power law with exponent 1.8 ± 0.2 and 2.7 ± 0.2 in the thin and thick target models, respectively, if $He^3/H = 5 \cdot 10^{-5}$. Thus, the slope of the proton spectrum agrees in general with the data of the interplanetary observations. For the thick target model, the total number of protons with energy $\gtrsim 30$ MeV was found to be $\sim 10^{33}$.

In connection with optical flares, heating by energetic electrons has been considered on several occasions (for example,[117,118]). For comparison of the penetrating capacity of thermal electrons (more precisely, of the stationary heat flux[41]), energetic electrons, and pro-

TABLE III. Flare heating of the chromosphere.

Quiet chromosphere in model of[136]				Region of H_α emission in flares in accordance with Table I in[46]	Heating agent					
					Heat flux		Energetic particles		Emission	
h, km	n_H, cm^{-3}	T, 10^3 °K	ξ, cm^{-2}		p=const	n=const	Electrons, E_e, keV	Protons, E_p, MeV	x ray, E_x, keV	Ultraviolet, A
					T_0, 10^7 °K					
1250	$5 \cdot 10^{12}$	6.4	$8.7 \cdot 10^{19}$		1		23	1.2	0.17	
1150	10^{13}	6.3	$1.7 \cdot 10^{20}$			~ 1	32	1.7	0.21	
1050	$2 \cdot 10^{13}$	6.1	$3.8 \cdot 10^{20}$		2		48	2.5	0.29	
1000	$3 \cdot 10^{13}$	6.0	$4.6 \cdot 10^{20}$				53	2.8	0.31	
950	$5 \cdot 10^{13}$	5.8	$5.3 \cdot 10^{20}$				56	3.0	0.33	
880	$8 \cdot 10^{13}$	5.6	$9.0 \cdot 10^{20}$	$\left.\right\}$ H_α (880–550)	3	~ 2	73	3.9	0.42	
820	10^{14}	5.3	$1.7 \cdot 10^{21}$			~ 3	100	5.3	0.68	
600	10^{15}	4.3	$1.1 \cdot 10^{22}$				260	14	1.4	
550	$2 \cdot 10^{15}$	4.2	$1.8 \cdot 10^{22}$				330	17	1.7	> 912
510	$3 \cdot 10^{15}$	4.1	$2.7 \cdot 10^{22}$				400	22	2.1	

tons, Table III contains the calculated values of the initial energy of particles that is needed if they are to traverse a thickness ξ (cm^{-2}) into the chromosphere; here h (km), T (10^3 K) and n_H (cm^{-3}) are the height above the photosphere, the temperature, and the hydrogen concentration in the model of the quiet chromosphere.[136]

It is clear that nonrelativistic protons with an energy approximately $\sqrt{m_p/m_e} \simeq 50$ times higher than the energy of the nonrelativistic electrons penetrate to the same depth as the electrons. The energy losses of such protons per unit thickness of matter is approximately the same number of times greater than for the corresponding electrons. Therefore, a proton flux $\sqrt{m_p/m_e}$ times smaller in number than the electron flux but with proton energy $\sqrt{m_p/m_e}$ times greater carries the same total energy and gives rise to the same heating of the atmosphere as the electron flux. The following difference is however important. Beginning at a depth corresponding to a matter thickness of about $3 \cdot 10^{22}$ cm^{-2} or a concentration $n_H \simeq 3 \cdot 10^{15}$ cm^{-3} and below, the heating of the chromosphere requires electrons with an energy above 400 keV, i.e., electrons for which a relativistic behavior of the losses becomes important. Protons that have penetrated to the same depth have essentially nonrelativistic energies $E_p \gtrsim 20$ MeV. It could be this that explains why all white-light flares, i.e., having flare kernels with enhanced optical continuum, have been observed to be proton flares.[137] However, whether there is here a rigorous one-to-one correspondence is at present not known. At the same time, it is known that during the 3*B* flare on August 7, 1972 two forms of continuum optical emission were observed.[138,139] The first of them consisted of short-lived compact blue-white kernels observed at approximately the same time (1519–1524 UT) as the protons were accelerated.[140] The second was a long-lived diffuse moving yellow-white front that coincided with the leading edge of the H_α emitting ribbon. Simultaneously, a slow drift of the maximum of the microwave emission to lower frequencies was observed, and the spectrum of the nonthermal x-ray emission became softer.

Rust and Hegwer[139] pointed out the intimate connection between the continuum optical, microwave, and hard x-ray emissions and suggested that both forms of white emission were due to heating of the chromosphere by the same energetic electrons as generated the hard x rays and the microwave radio emission. Thus, to explain a white-light flare there is no need to invoke heating by energetic protons. Moreover, one gets the impression that, in contrast to electrons, energetic protons escape virtually freely from the acceleration region into interplanetary space (see, for example,[141]) and cannot guarantee the heating of the chromosphere necessary for a white-light flare. According to the interpretation of[142] of the gamma emission with energy above 300 keV, the total energy of the protons in the thick target is less than 10^{28} erg, i.e., clearly inadequate for a white-light flare.

4. GAS DYNAMIC PHENOMENA IN THE ATMOSPHERE OF THE SUN

A. Optical flare as response of the chromosphere to a shock wave

Thus, during a solar flare a number of processes can lead to local heating of the corona and the chromosphere to high temperatures. At the boundary of the hot region there then arise large temperature and pressure gradients. They must lead to rapid gas-dynamic motions and shock waves. It is assumed that a shock wave propagating into the chromosphere is the cause of the optical emission of the flare and the observed sequence of excitation of lines observed by the profiles of the lines, the continuum emission, and other features.[143–147] Shock waves can be excited, for example, at places where matter falls onto the chromosphere from the corona[143,144] or there is heating of the atmosphere by energetic electrons.[146,147] According to[8,9], the basis of the explosive phase of the flare is the breaking of the current sheet. The "gap" formed in the sheet expands with Alfvén velocity; at the same time, there is induced in the sheet an impulsive electric field that accelerates the charged particles and gives rise to turbulent heating of the plasma in the region of the break. But it is obvious that an appreciable fraction of the energy liberated during the break is transformed into the energy of magnetohydrodynamic motions, i.e., ejections of plasma and shock waves. Thus, the shock wave may be due to rearrangement of the magnetic field in the corona during the explosive phase of the flare.

The depth of penetration of a strong shock wave into the chromosphere can be estimated by means of the well-known self-similar solution in an exponential atmosphere[148] if one ignores emission losses. A shock wave with initial Mach number $\mathbf{M}$ becomes weak ($\mathbf{M} \to 1$) after it has traversed the path

$$\Delta h \equiv h_2 - h_1 \simeq C h_0 \ln \mathbf{M}; \tag{4.1}$$

Here h_0 is the height of the homogeneous atmosphere, and the factor C depends on the adiabatic exponent and differs little from unity. If the shock wave arises as a result of heating of electrons with energy about 10 keV, i.e., at a height h_1 above the photosphere, where the hydrogen concentration is $n_H \simeq 10^{12}$ cm^{-3}, then for $\mathbf{M} = 10$–30 this shock wave can reach a height h_2, where $n_H \simeq 10^{13}$–$3 \cdot 10^{13}$ cm^{-3}, respectively.

Thus, the shock wave propagating into the chromosphere is very rapidly damped because of the exponential growth of the density and pressure in front of the shock and the rapid decrease of the pressure behind the front because of the movement upward of heated matter. The depth of penetration of the shock wave into the chromosphere may be appreciably greater than the depth determined by Eq. (4.1) if the injection of energy behind the front continues a long time, as, for example, in the case of heating of the chromosphere by a stationary stream of energetic electrons for 100 sec (see[146,147]). There are however reasons to believe (see below) that the duration of heating of each given section of the chromosphere is appreciably shorter, and the flux of particles has the nature of short bursts that reach different sections of the chromosphere.

B. Influence of emission on the propagation of the shock wave. Thermal instability behind the shock front

Emission losses obviously reduce the depth of penetration of a shock wave into the chromosphere. This conclusion is confirmed by the numerical calculation of[145], in which it is assumed that the gas heated behind the shock front is optically thin and that its emission losses are proportional to T^3 for $T \leqslant 5 \cdot 10^4$ °K and $T^{3.5}$ for $T \leqslant 2.5 \cdot 10^5$ °K.

In[149], Guseĭnov, Imshennik, and Paleĭchik considered a model of the initial phase of chromospheric flare in the framework of the theory of a high-temperature explosion in a homogeneous atmosphere. They solved numerically the one-dimensional system of the equations of the gas dynamics of an ionized two-temperature plasma with allowance for all significant dissipative processes. This made it possible to describe the structure of the front of the shock wave, take into account the difference between the electron and ion temperatures, and also radiative cooling of the hot gas behind the shock front. The dependence of the volume emission on the temperature was taken from[150] and was characterized by the presence of a maximum. The calculations showed that the volume emission leads to a thermal instability of the hot plasma behind the shock front. The plasma is rapidly cooled by the emission and is compressed into cold dense layers. Similar results were obtained in[151].

In connection with protuberances on the Sun and in a larger plan the phenomenon of thermal instability has long been known.[152,153] A linear theory of thermal instability was constructed in[154] by Field. (Below, using equations from[145], we shall place the letter F in front of the corresponding equation numbers.) The theory was developed further and has found numerous applications (see, for example,[155-157]). In the linear theory, the homogeneous medium in thermal and mechanical equilibrium is characterized by three dimensionless parameters α, β, and γ. The first two are the ratios (F.27) of the characteristic values of the wave numbers (F.16) that determine the emission and heat conduction losses, and the third is simply the ratio of the specific heats, which we assume is constant.

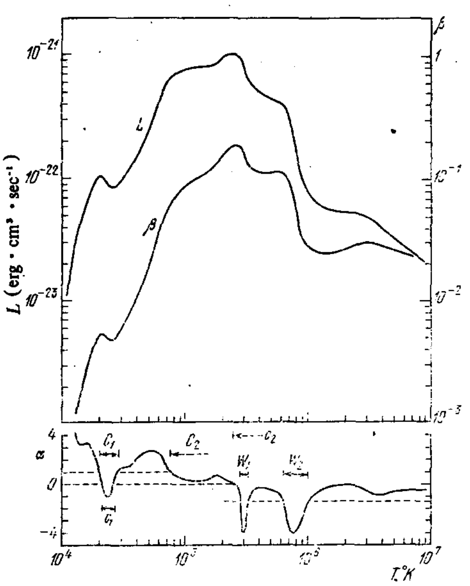

FIG. 8. Radiative cooling function $L(T)$ in erg · cm³ · sec⁻¹ calculated by Cox and Tucker.[158] The temperature-dependent dimensionless parameters of the medium are α and β. The instability regions of the different modes of thermal instability are shown.

If the heating of the medium is such that the supply of energy per gram of matter per second does not depend on the temperature and density, and the cooling of the medium is determined by the volume emission losses (1.5), then the parameter α depends only on the temperature and is the logarithmic derivative of the radiative cooling function

$$\alpha(T) = \frac{d \ln L}{d \ln T}. \tag{4.2}$$

The parameter β characterizes the relative importance of heat conduction. If the heat conduction is determined by free electrons, i.e., $\varkappa_e \simeq \varkappa_0 T^{5/2}$, then

$$\beta(T) = \frac{(\gamma-1)^2}{\gamma} \frac{\mu\varkappa_0}{R^3} \sqrt{T}\, L(T) \tag{4.3}$$

also depends only on the temperature; here, μ is the effective molecular weight (for a plasma with cosmic abundance of the elements, $\mu \simeq 1.44 m_{\mathrm{H}}$), R is Boltzmann's constant, and $\varkappa_0 \simeq 1.45 \cdot 10^{-6}$.

For a plasma with cosmic abundance of the element, the radiative cooling function $L(T)$ was calculated by Cox and Tucker[158] and is shown in Fig. 8 together with the functions $\alpha(T)$ and $\beta(T)$. To calculate β in accordance with Eq. (4.3) $\gamma = 5/3$ was assumed. Figure 8 also shows the temperature regions in which perturbations of the following types may be unstable: 1) *Isobaric* perturbations, i.e., perturbations for which $p = \mathrm{const}$. They correspond to two regions C_1 and C_2 in which $\alpha < 1$. This is the so-called condensation mode of the thermal instability. 2) *Adiabatic* perturbations (with constant entropy) are unstable in the regions W_1 and W_2, where $\alpha < -3/2$. This mode of the thermal instability is called the *acoustic* or *wave* mode. 3) *Isochoric* ($n = \mathrm{const}$) perturbations are unstable in the regions c_1 and c_2, where $\alpha < 0$ (see[152]).

We introduce instead of the characteristic values of the wave numbers (F.16) the matter thicknesses corresponding to them:

$$\xi_\rho = \frac{n}{k_\rho} = \frac{\gamma^{1/2}}{\gamma-1} \frac{R^{3/2}}{\mu^{1/2}} \frac{T^{3/2}}{L(T)}, \qquad \xi_T = \frac{n}{k_T} = \alpha^{-1}\xi_\rho, \quad \xi_\varkappa = \frac{n}{k_\varkappa} = \beta\xi_\rho. \tag{4.4}$$

The thermal instability is stabilized by heat conduction over scales smaller than the critical value (F.26) of the matter thickness:

$$\xi_c = \xi_\rho \beta^{1/2} (1-\alpha)^{-1/2} \tag{4.5a}$$

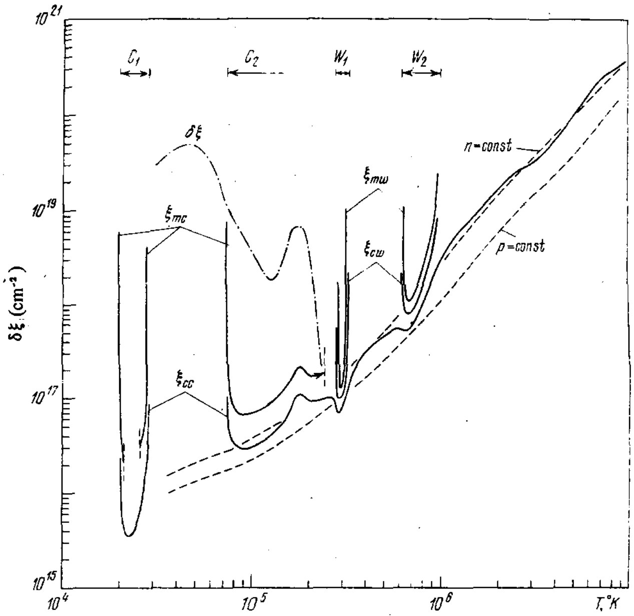

FIG. 9. Scales of perturbations of condensation ξ_{cc} and acoustic ξ_{cw} type stabilized by heat conduction (see (4.5)) and also scales of perturbations that have the largest growth rate, ξ_{mc} and ξ_{mw} (see (4.7)). The dashed curves show the characteristic thicknesses for the temperature profiles in the case of stationary heating of the chromosphere by a heat flux[41] in the two limiting cases p = const and n = const. The dot-dash-dot curve shows the characteristic thicknesses for the temperature profile in Fig. 10.

and

$$\xi_c = \xi_\rho \beta^{1/2} \left(-\alpha - \frac{1}{\gamma - 1}\right)^{-1/2} \tag{4.5b}$$

for the condensation and acoustic modes, respectively. These values of the thickness also depend only on the temperature and are shown in Fig. 9.

As above, we shall consider one-dimensional equilibrium distributions of the temperature $T(\xi)$ produced by some mechanism of heating of the solar plasma in the presence of volume cooling by emission. We shall compare the characteristic thicknesses

$$\delta\xi(T) = \frac{d\xi(T)}{d \ln T}, \tag{4.6}$$

over which the temperature changes appreciably along such a profile with the characteristic thickness (4.5) for perturbations in a homogeneous medium. As an example, the dashed lines in Fig. 9 are the characteristic thicknesses for the temperature profiles corresponding to stationary heating of the chromosphere by a heat flux in the two limiting cases p = const and n = const.[41] At every point of such a temperature profile, there is a balance between heating by the heat flux and the emission losses. It can be seen from Fig. 9 that in both limiting cases the temperature profiles are stable against perturbations whose scale is less than $\delta\xi$. For scales greater than or comparable with $\delta\xi$, the approximation of a homogeneous medium does not apply.

The greatest growth rate of the thermal instability corresponds to the characteristic thicknesses (F.46):

$$\xi_m = \left[\frac{(1-\alpha)^2}{\gamma^2} + \frac{\alpha(1-\alpha)}{\gamma}\right]^{-1/4} (\xi_\rho \xi_c)^{1/2} \tag{4.7a}$$

and

$$\xi_m = \left|\frac{\alpha - 1}{\gamma}\right|^{-1/2} (\xi_\rho \xi_c)^{1/2} \tag{4.7b}$$

for the condensation and acoustic modes, respectively, and they are also shown in Fig. 9.

In the problem of a strong explosion in a homogeneous atmosphere[149] the temperature behind the shock front at the initial times is very high: 10^6–10^8 °K. Because of the high thermal conductivity, the thermal instability can be manifested here only over very large thickness scales: $\delta\xi > \xi_c$ in Fig. 9. But compression (condensation) of matter on such a scale requires a considerable time $t_s \simeq \delta\xi / n V_s$, where V_s is the velocity of sound behind the shock front. With expansion of the strong shock sphere, the temperature falls behind the shock front, the permitted thickness scale decreases and the characteristic compression time shortens, and the rate of radiative cooling increases as the maximum of the function $L(T)$ is approached (see Fig. 8). Therefore, after a certain time the matter behind the shock front is condensed into cold dense layers.

In connection with solar flares, the possibility of thermal instability behind a shock front was first pointed out in[149]. Under the conditions of solar flares, the thermal instability can develop in a very short time: 10^{-1}–10^{-2} sec, as will be shown below. Weymann,[153] considered as long ago as 1960 the stationary heating of the chromospheres of stars by shock waves and was the first to give the correct criterion for condensation thermal instability. Kostyuk and Pikel'ner[146] formulated the problem of the formation and propagation of a shock wave in the case of prolonged (≃ 100 sec) stationary heating of the chromosphere by a stream of energetic electrons with power-law spectrum. They considered the one-dimensional system of equations of gas dynamics with heat conduction by electrons and neutrals, ion viscosity,[147] and radiative cooling. However, in the numerical calculation they did not foresee the possibility of the appearance and rapid development of thermal instability. It was assumed that the problem contains no characteristic times shorter than 1 sec (the calculation step). On the basis of this, they did not, in particular, consider the possibility of the electron temperature becoming different from the ion temperature. Taken as a whole, the gas-dynamic picture of a solar flare is more complicated than the picture considered in[146,147] for several reasons. First, as is shown by modern observations (for example, [105,106,123,138,139]) the injection of energetic electrons into the chromosphere takes the form of successive short (of a few seconds) pulses, which partly overlap in time, so that the illusion of continuity was created when the time resolution was poor. These pulses correspond to different points on the chromosphere. Second, the prolonged quasistationary heating of the chromosphere in, for example, the flare ribbons is evidently due not to energetic particles but heat fluxes from the region of rejoining of the magnetic field, and it also takes place along different lines of force. This is indicated, for example, by the motion of the flare ribbons in opposite directions from the zero line of the photospheric magnetic field. Third, in the case of flare heating of the chromosphere the thermal instability may begin before the occurrence of the shock wave and strongly influence the gas-dynamic picture of the flare.

C. Thermal instability of a hot flare plasma before formation of the shock wave

The hot ($T > 2\cdot 10^4\,°$K) flare plasma is usually virtually transparent for its own emission. The cooling of the plasma by emission has a volume nature. During the flare heating, it restricts the growth of the temperature and leads to the formation of quasiequilibrium distributions of the temperature and the density which are, in general, unstable against perturbations of the thermal or mechanical equilibrium.

Let us consider as an example the heating of the chromosphere by electrons accelerated in the flare with the power-law spectrum (3.2). The power released by the electron beam as a result of Coulomb losses in a plasma with concentration $n(s)$ cm^{-3} distributed over the thickness ξ cm^{-2} in accordance with Eq. (1.4), in which the function $P(\xi)$ in the general case is expressed in terms of Gaussian hypergeometric functions (see Eq. (12) in[64]). Suppose, to be specific, that the exponent of the differential spectrum of the particle flux is $\gamma = 3$, i.e., the spectrum is hard, and the upper end of the spectrum is at $E_2 = \infty$. Then

$$P(\xi) = \Pi\left(\frac{\xi}{\xi_1}\right)^{-3/2}\Lambda\left(\frac{\xi}{\xi_1}\right), \tag{4.8}$$

where $\Pi = aF_0/2E_1^2$ is a constant, $\xi_1 = E_1^2/2a$ is the characteristic thickness over which an electron with initial energy E_1 loses its energy, and

$$\Lambda\left(\frac{\xi}{\xi_1}\right) = \begin{cases} (\pi/2) - \operatorname{arctg}\sqrt{(\xi_1/\xi) - 1} - (\xi/\xi_1)\sqrt{(\xi_1/\xi) - 1} & \text{for } \xi \leqslant \xi_1, \\ \dfrac{\pi}{2} & \text{for } \xi > \xi_1. \end{cases} \tag{4.9}$$

We shall assume that the boundary energy flux is sufficiently large that during the heating time

$$t_h(T(\xi)) = \frac{3k\,[T(\xi) - T_\infty(\xi)]}{P(\xi)} \tag{4.10}$$

the initial density distribution $n_\infty(\xi)$ does not have time to change. In other words, t_h is much shorter than the characteristic gas-dynamic time

$$t_g(T(\xi)) = \frac{\delta\xi}{n(\xi)\,V_S(T(\xi))}; \tag{4.11}$$

where $\delta\xi$ is the characteristic thickness (4.6) over which the temperature changes significantly and V_S is the velocity of sound for the temperature at the corresponding point ξ.

In addition, we shall assume that the heat conduction does not affect the establishment of an equilibrium distribution of the temperature $T(\xi)$, i.e., the heating time is much shorter than the characteristic heat conduction time

$$t_c(T(\xi)) = \frac{3k\,(\delta\xi)^2}{n(\xi)\,\varkappa(T(\xi))}; \tag{4.12}$$

here $\varkappa(T)$ is the electron thermal conductivity, since in the range of temperatures $T \gtrsim 2\cdot 10^4\,°$K and concentrations $n < 10^{15}$ cm^{-3} in which we are interested the hydrogen is almost completely ionized.

Under these assumptions one can establish the quasi-equilibrium temperature distribution, which is determined by equality of the heating by energetic electrons (4.6) and the volume emission cooling:

$$\Pi\left(\frac{\xi}{\xi_1}\right)^{-3/2}\Lambda\left(\frac{\xi}{\xi_1}\right) = n_e L(T(\xi)); \tag{4.13}$$

here, we have ignored the heat source $\mathcal{F}_\infty(T_\infty, n_\infty)$ that maintains the original temperature distribution in the quiet chromosphere (cf. Eqs. (2.1) and (3.21)).

The cooling by emission is capable of equalizing the heating by electrons only if one is sufficiently deep in the chromosphere, namely, for $\xi > \xi_m$, where the smallest value of ξ is determined by the obvious condition

$$L_M n_\infty(\xi_m) = P(\xi_m), \tag{4.14}$$

with $L_M \equiv \max L(T) = L(2.5\cdot 10^5\,°\mathrm{K}) \simeq 1.05\cdot 10^{21}$ erg $\cdot$ cm^3 $\cdot$ sec^{-1}. The equilibrium temperature distribution corresponding to heating by electrons with spectral parameters $F_0 = 10^{11}$ erg $\cdot$ cm^{-2} $\cdot$ sec^{-1}, $E_1 = 10$ keV, $E_2 = \infty$, and $\gamma = 3$ is shown in Fig. 10 together with the characteristic times (4.10)–(4.12). For simplicity, the real density distribution in the region of the chromosphere in which we are interested has been replaced by an exponential distribution with scale height $h_0 = 200$ keV:

$$n_\infty(\xi) = h_0^{-1}\xi\ (\mathrm{cm}^{-3}). \tag{4.15}$$

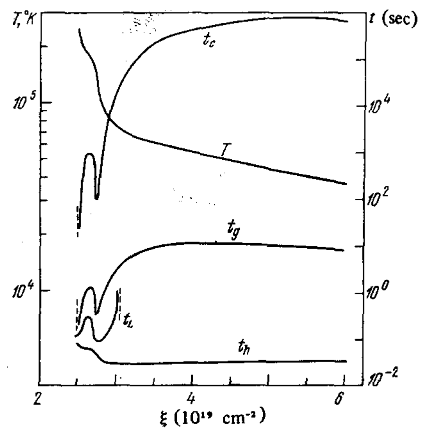

FIG. 10. Distribution of the temperature T over the thickness ξ (cm^{-2}) into the chromosphere when the heating by energetic electrons ($\gamma = 3$, $F_0 = 10^{11}$ erg $\cdot$ cm^{-2} $\cdot$ sec^{-1}, $E_1 = 10$ keV, $E_2 = \infty$) is balanced by radiative cooling. The characteristic heating time is t_h; the time of development of the thermal instability is t_L in the regime p = const; the time of stabilization of the instability by heat conduction is t_c and the characteristic gas-dynamic time is t_g.

The calculated equilibrium temperature distribution $T(\xi)$ corresponds to the characteristic thicknesses $\delta\xi$ (4.6), which characterize the inhomogeneity scale of the temperature profile and are shown in Fig. 9 by the dot-dash-dot curve. It is obvious that in the range of temperatures from $8 \cdot 10^4$ to $2 \cdot 10^5$ °K the equilibrium distribution of the temperature is virtually homogeneous with respect to the perturbations that have the greatest growth rate, i.e., perturbations with characteristic matter thickness ξ_{mc} (4.7a). Therefore, in this range of temperatures one can use the results of the linear theory of the thermal instability in a homogeneous medium. For example, ignoring heat conduction and considering gas-dynamic compression in the constant pressure regime, we can write down for the characteristic time of development of the condensation mode the simple expression

$$t_L(p = \mathrm{const}) = \frac{5kTh_0}{(1-\alpha)\,L(T)\,\xi}. \tag{4.16}$$

Since $\xi_{mc} \ll \delta\xi$ there is of course no contradiction here between isobaric compression of condensation perturbations and isochoric heating to the equilibrium temperature. In accordance with the general linear theory[154] the formation of condensations begins in the region of temperatures where $\alpha < 1$, which corresponds to temperatures $T \geqslant 7.4 \cdot 10^4$ °K on Cox and Tucker's curve (Fig. 8). For comparison with the other characteristic times, t_L is shown as a function of ξ in Fig. 10.

Figure 10 shows that the time of heating of the chromosphere to the equilibrium temperature is shorter than the characteristic instability time, which in its turn is shorter than or comparable with the gas-dynamic time. Therefore, the instability may begin before or at the same time as the formation of the shock wave. In this respect too the picture considered here differs from the situation in which the heating and compression of the medium that leads to instability are due to the passage of a strong shock wave.[149,151] Figure 10 also shows that heat conduction does not succeed in stabilizing the thermal instability.

Under conditions of flare heating of the chromosphere, the thermal instability has a strong influence on the gas-dynamic picture of the flare for the further reason that the thermal instability may develop over a characteristic time that is determined by radiative cooling and is shorter than the characteristic gas-dynamic time. In the example considered, the characteristic time of the condensation mode is shorter than or comparable with the characteristic gas-dynamic time, which ensures condensation of the matter cooled by the emission in a nearly $p = \mathrm{const}$ regime. As a result, if the chromosphere is heated by a sufficiently powerful stream of energetic electrons, dense cold layers or filaments must arise, at least during the start of the process, and their presence will influence the nature of the optical emission of the flare. Thus, rapid gas-dynamic motions and shock waves are inescapable consequences of sufficiently powerful liberation of energy in the atmosphere of the Sun. These processes take place in the presence of strong cooling by emission, which leads to thermal instability—the formation of dense cold layers of gas that influence the gas-dynamic picture of the flare and especially its emission. A self-consistent treatment of these phenomena requires simultaneous solution of the equations of gas dynamics, radiative transfer, and ionization equilibrium in, for example, the approximation described in[159].

5. HEATING OF THE SOLAR ATMOSPHERE BY THE EMISSION OF THE HOT REGION OF THE FLARE

A. Specific features of heating by radiation

The overwhelming part (from 90 to 99%) of the total flare emission energy lies in the soft x-ray and ultraviolet ranges of the hot flare region. A major part of the radiation of the hot region escapes from it into interplanetary space. Having been partly absorbed in the source itself and during propagation, this radiation reaches the ionosphere of the Earth, where it causes a rapid rise in the ionization, which is observed, for example, in the frequency drift of reflected radio waves.[137,160]

Below, we shall be interested in the emission of the hot flare region that does not escape from the solar atmosphere but is absorbed in it, giving rise to additional ionization and ultimately heat. Thus, an appreciable part of the emission is absorbed in the chromosphere directly under the hot region and in the immediate neighborhood. This radiation can change the structure of the flare transition layer and increase the optical emission of the flare.

An important feature of the radiative transfer of the energy is that the radiation escapes from the hot region isotropically and not along the tubes of magnetic lines of force, as is the case for the heat fluxes and the energetic particles. It is therefore probable that the energetic particles and the heat fluxes generate flare kernels, knots, ribbons, and other bright compact formations within less bright and diffuse regions (halo) heated by the emission of the hot region. The efficiency of radiative heating obviously depends strongly on the geometry of the high-temperature region, especially its height.

In contrast to shock and heat waves and also nonrelativistic particles, radiative transfer of energy does not introduce an additional (relative to the velocity of light) time delay. Therefore, the radiative transfer of energy certainly does not contradict the observed simultaneity of the phenomena that take place during the flare at different heights (see, for example,[54,123]).

Finally, and this is the most important thing, the emission of the hot flare region has a high capacity to penetrate. If we assume, following Table I in[46], that the hydrogen concentration in the region of formation of the flare H_α emission is $n_H = 5 \cdot 10^{13}-2 \cdot 10^{15}$ cm^{-3} (in the quiet chromosphere,[136] the H_α emission is formed in the range of hydrogen concentrations $n_H \simeq 7 \cdot 10^{11}-2 \cdot 10^{16}$ cm^{-3}; see Fig. 5) which corresponds to a thickness $\xi \approx 7 \cdot 10^{20}-2 \cdot 10^{22}$ cm^{-2}, then for penetration to this region we need (see Table III) electrons with energies $E_e = 70-300$ keV or protons with energies $E_p = 4-20$ MeV, or x rays with energies of only $E_x = 0.4-1.8$

keV, or ultraviolet rays in the region $\lambda > 912$ Å (see Fig. 2 in[161]).

B. X-ray heating of the solar atmosphere

That x rays can give rise to appreciable heating of the optical region of the flare can be readily seen without recourse to the model calculations[45,78] made for the thermal x-ray emission with the elementary spectra (2.5).

Let us consider as an example the large flare on August 7, 1972 at 1515 UT. At the maximum of this flare, the softest channel 8–20 Å of x-ray detectors on the satellites Solrad 9 and 10 was saturated.[162] This means that the energy flux of the x rays in the range 0.6–1.5 keV exceeded 1 erg · cm^{-2} sec^{-1} at the Earth. Therefore, the power of the x-ray source on the Sun was not less than $3 \cdot 10^{27}$ erg · sec^{-1} in this range. If it is assumed that about 1/3 of this emission is absorbed in the chromosphere, then, given a flare area of about $3 \cdot 10^{19}$ cm^2, the energy flux density of the x rays directed into the chromosphere was not less than $3 \cdot 10^7$ erg · cm^{-2} sec^{-1}. Attenuated by about e times on the propagation path, this flux could give rise to a density of H_α radiation up to 10^7 erg · cm^{-2} sec^{-1}, i.e., approximately the same as that due to heat conduction within the flare kernels at $T_0 \doteq 3 \cdot 10^7$ °K.

Calculations of the absorption of the thermal x-ray emission in the atmosphere of the Sun[78,45] revealed some interesting features.

First, up to 30% of the x-ray emission of the flare, and moreover the softest, can be absorbed in the emission source. Therefore, the opacity of the x-ray source in the region of the softest x rays may be important for the interpretation of the observed spectra.

Second, the emission of elementary tubes with boundary temperature $T_0 < 10^7$ °K is absorbed mainly above the region in which the flare H_α emission is formed. We should enter the caveat that the uncertainty is too large in the determination of the parameters of this region. It is possible that the H_α flare is formed higher in the chromosphere than assumed here.

Third, only an insignificant part ($\lesssim 1\%$) of the x-ray energy flux directed downward may reach the photosphere even in the case of boundary temperatures as high as $5 \cdot 10^7$ °K.

Finally, and this is the most important, about 30% of the x-ray flux is absorbed in the region of the H_α flare if $10^7 \lesssim T_0 \lesssim 3 \cdot 10^7$ °K. Moreover, the higher the boundary temperature T_0 the larger the fraction ($\geqslant 30\%$ for $T_0 \geqslant 3 \cdot 10^7$ °K) is the flux of x-ray energy that penetrates to the region of the chromosphere with hydrogen concentration $n_{\rm H} \gtrsim 2 \cdot 10^{15}$, where, probably, the continuum optical emission is formed in all white-light flares. Therefore, to construct models of white-light flares it may be necessary to take into account the mechanism of x-ray heating of the source of the white continuum.

In connection with x-ray heating, it is also appropriate to discuss how one can deduce from observations an important flare parameter such as the energy flux F_0 in the flare kernels.

One can attempt to answer this question by considering the simplest model situations. For example, if observations of hard x-ray bursts have enabled us to find the power $\mathscr{F}$ of the stream of energetic electrons, then under the assumption that these electrons are the principal source of heating of the flare plasma, one can estimate the boundary energy flux as $F_0 = \mathscr{F}/S_1$. Here, S_1 is the area of the flare kernels, which in accordance with the observations[54,79,80] is much less than the total area of the flare—the area S_2 of the flare halo. Knowing F_0 we can, for example, calculate the heating of the flare halo by x rays, as was done in[45,78]. However, the total power $\mathscr{F}$ of the nonthermal electrons is usually unknown since the lower limit E_1 of their energy spectrum is not known. Therefore, one can in principle consider the opposite problem; namely, assuming that the H_α emission in the halo is due to x-ray heating, estimate the necessary power of the x-ray source and the boundary energy flux needed for the existence of such a source.

Thus, the boundary flux F_0 can be estimated if it is assumed that the diffuse halo of the optical flare is heated by the x-ray emission of the hot region. However, it must be borne in mind that a comparable, if not larger, contribution to the heating of the upper chromosphere may be made by the ultraviolet emission in the region of the Lyman continuum ($\lambda \leqslant 912$ Å), which is formed in the flare transition layer.

There exist some other possibilities for determining the boundary energy flux F_0 in the flare kernels, where the greatest energy liberation power is observed. For example, one can estimate F_0 from the known temperature T_0 and concentration n_0 in the high-temperature region by assuming constancy of the pressure or constancy of the density along the magnetic tubes through which the energy reaches the flare kernels. Another way of estimating the boundary energy flux is to proceed from the observed intensity of H_α emission in the flare kernels $F(H_\alpha)$. In this case $F_0 \simeq 10^2 F(H_\alpha)$ in the case of heating by heat conduction or $F_0 \simeq (10–30) F(H_\alpha)$ in the case of heating by energetic electrons (see Table II).

All the above ways of estimating the boundary energy flux are however indirect and inaccurate. It would be more direct and accurate to find the boundary energy flux in all flare kernels by first determining the lower limit E_1 of the energy spectrum of the accelerated electrons, since they are evidently the main source of heating in the kernels. For this it is necessary to regard the power $\mathscr{F}(E > E_1)$ of the energetic electrons calculated by means of Eq. (3.12) or (3.13) from the data on the spectrum of the hard x-ray emission as a function of E_1 and equate it to the total power of the emission in all the flare kernels. Of particular importance here is the impulsive component of the ultraviolet, soft x ray, the optical continuum (if it is observed) emissions since in them the observed power is maximal.

C. Heating by ultraviolet emission of the flare

The ultraviolet emission of a flare contains energy that is almost an order of magnitude greater than in the x rays.[163] Therefore, during the time of large flares the energy flux of the ultraviolet radiation may reach several erg · cm^{-2} · sec^{-1} at the Earth[137,164] and accordingly about 10^8 erg · cm^2 · sec^{-1} deep in the chromosphere. If it is assumed that the absorption of ultraviolet radiation in the chromosphere is determined by the same effective cross section as in interstellar gas with ordinary composition and temperature (see Fig. 2 in[161]), then two wavelength regions are distinguished by the nature of the absorption. The ultraviolet radiation in the region of the Lyman continuum $\lambda \leq 912$ Å is absorbed mainly in the upper chromosphere itself for $\xi \gtrsim 10^{17}$ cm^{-2}. In contrast, radiation with $\lambda < 912$ Å penetrates deep into the chromosphere and is absorbed primarily at $\xi \gtrsim 2 \cdot 10^{22}$ cm^{-2}, i.e., in a region with hydrogen concentration $n_H \gtrsim 2 \cdot 10^{15}$ cm^{-3} (Table III).

At the maximum of the white-light flare on March 12, 1969 the energy flux of the ultraviolet emission in the band 760–1030 Å was about 4 erg · cm^{-2} · sec^{-1} at the Earth,[164] which corresponds to a power of not less than 10^{28} erg · sec^{-1} in this band or $5 \cdot 10^{27}$ erg · sec^{-1} in the band 912–1030 Å. Let us suppose that almost all this radiation was formed in the flare transition layer within the flare kernels. There were three such kernels in the flare on March 12, 1969 and they could be clearly seen both in H_α and in the optical continuum (see Fig. 4 in[137]). If the area of the kernels is taken to be $5 \cdot 10^{17}$ cm^2, then the radiation flux in the band 912–1030 Å in the region of the chromosphere with concentration $n_H > 2 \cdot 10^{15}$ cm^{-3} is approximately $6 \cdot 10^9$ erg · cm^{-2} · sec^{-1}, i.e., not much less than the flux needed to produce the continuum optical emission. It is probable that to explain a white-light flare it is necessary to take into account all ultraviolet radiation with wavelengths $\lambda > 912$ Å. At the same time, the continuum optical emission can be formed over an appreciable range of depths in the chromosphere: many layers of the chromosphere, each with its own temperature and dominant opacity mechanism, contribute in this case to the white continuum.

6. CONCLUSIONS

The problem of investigating the extremely complicated and ramified process of a solar flare can be divided rather naturally into two parts, which may be called the internal and external problems. The first of them corresponds to the investigation of the primary physical process as a result of which a tremendous amount of energy is liberated in a short period of a few tens of seconds in the form of massive hydrodynamic motions, fluxes of accelerated particles, and fluxes of heat and radiation. This process is obviously the basis for understanding the flare, and its investigation is the most important part of theory. However, information about this process can be obtained only by a very indirect manner, mainly from the rather distant consequences that it has in the atmosphere of the Sun, the interplanetary medium, and on the Earth. In addition, these secondary effects by themselves have an important significance for astrophysics, the physics of interplanetary space, and geophysics. Therefore, the external problem plays a very important role. Its main aim is to investigate the secondary effects of flares. The main effects are associated with the response of the solar atmosphere to the energy fluxes that arise in the primary flare process.

The study of the flare mechanisms of heating and other secondary processes in the chromosphere and corona gives one in principle the possibility of obtaining detailed information about the primary flare process. This problem is complicated and not always unambiguous. Nevertheless, there are now a number of important results that significantly deepen our understanding of the flare process, and in some respects force us to reexamine this phenomenon. Such results are the following.

First of all, it has become clear that the traditional picture of a flare as a brightening (basically in the hydrogen line H_α) of part of the chromosphere relates to only one of the late consequences of the primary physical process.

In this connection, one should emphasize two circumstances, which significantly change our previous ideas about flares.

First, energetically the emission in H_α is only a few percent of the total power of the flare and in this respect is not a sufficiently adequate characteristic of the flare as a source of disturbances on the Sun, in the interplanetary medium, and on the Earth. The overwhelming part of the energy is released in the form of mass motions and accelerated particles, and also in the ultraviolet and soft x-ray spectral ranges.

Second, a flare, if one has in mind its principal process, is specifically a coronal and not chromospheric phenomenon. This is clear alone from the relative importance of the ultraviolet and x-ray emissions. In this connection, the very term chromospheric flare, which is usually used for the phenomenon as a whole, is not very felicitous.

Apart from these general conclusions of qualitative character, the investigation of the "external" problem already enables us to determine now important parameters of the primary process such as the total flux of energy expended on heating the solar atmosphere, the fraction of this flux due to energetic particles and radiation, the importance of rapid motions and shock waves, the space-time structure of flares, etc.

There is every reason to hope that further investigations of these channels through which the energy of the primary process of the flare reaches the atmosphere of the Sun and the analysis of the concomitant physical processes will not only make it possible to systematize the considerable amount of accumulated observational material but will also cast new light on this remarkable phenomenon of nature.

[1] A. M. Ellison, The Sun and Its Influence, Routledge, London (1955).
[2] C. de Jager, Structure and Dynamics of the Solar Atmosphere, Handb. Phys. Vol. 52, Springer-Verlag, Berlin (1959), p. 80.
[3] H. J. Smith and E. P. Smith, Solar Flares, Macmillan, London, Collier-Macmillan, New York (1963).
[4] A. B. Severny, Ann. Rev. Astron. and Astrophys. 2, 363 (1964).
[5] Z. Švestka, Solar Flare, D. Reidal, Dordrecht (1976).
[6] Collected Data Reports on August 1972 Solar–Terrestrial

Events, Vols. 1–3, Ed. H. E. Coffey, World Data Center A, Rept. UAG-28 (1973).
[7]V. L. Ginzburg and S. I. Syrovatskiĭ, Proiskhozhdenie Kosmicheskikh Lucheĭ (The Origin of Cosmic Rays), Nauka, Moscow (1963); see also the corrected and enlarged English edition: V. L. Ginzburg and S. I. Syrovatskiĭ, The Origin of Cosmic Rays, Pergamon Press (1964).
[8]S. I. Syrovatskii, Izv. Akad. Nauk SSSR, Ser. Fiz. (1975); in: Tr. VII Leningradskogo Mezhdunarodnogo Seminara "Korpuskulyarnye Potoki Solntsa i Radiatsionnye Poyasa Zemli i Yupitera," Leningrad (Proc. Seventh Leningrad International Seminar "Corpuscular Solar Fluxes and the Radiation Belts of the Earth and Jupiter," Leningrad), Leningrad Institute of Nuclear Physics (1975), p. 63.
[9]Neĭtral'nye Tokovye Sloi v Plazme (Neutral Current Sheets in Plasmas), Tr. Fiz. Inst. Akad. Nauk SSSR 74 (1974).
[10]S. I. Syrovatskiĭ, *ibid*. p. 3.
[11]S. V. Bulanov and S. I. Syrovatskiĭ, *ibid*. p. 88.
[12]B. B. Kadomtsev, Fiz. Plazmy, 1, 710 (1975).
[13]A. A. Galeev and L. M. Zelenyĭ, Zh. Eksp. Teor. Fiz. **69**, 882 (1975). [Sov. Phys. JETP 42, 450 (1975)].
[13a]S. B. Pikel'ner and V. N. Tsytovich, Astron. Zh. 52, 738 (1975) [Sov. Astron. 19, 450 (1975)].
[14]B. Coppi, Astrophys. J. **195**, 545 (1975).
[15]E. P. Priest and M. A. Raadu, Solar Phys. **43**, 177 (1975).
[16]N. I. Gerlakh and S. I. Syrovatskiĭ, quoted in the collection,[9] p. 73.
[17]B. V. Somov and S. I. Syrovatskiĭ, quoted in the collection,[9] p. 14.
[18]J. C. Stevenson, J. Plasma Phys. **7**, 293 (1972).
[19]S. Fukao and T. Tsuda, J. Plasma Phys. **9**, 409 (1973).
[20]E. R. Priest, Astrophys. J. **181**, 227 (1973).
[21]T. Yeh and M. Dryer, Astrophys. J. 182, 301 (1973).
[22]S. I. Syrovatskii, A. G. Frank, and A. Z. Khodzhaev, Pis'ma Zh. Eksp. Teor. Fiz. 15, 138 (1972) [JETP Lett. 15, 94 (1972)].
[23]S. Yu. Bogdanov, N. P. Tokarevskaya, A. G. Frank, and A. Z. Khodzhaev, Fiz. Plazmy 1, 133 (1975) [Sov. J. Plasma Phys. 1, 71 (1975)].
[24]G. V. Dreĭden, A. N. Zaĭdel', V. S. Markov, A. M. Mirzabekov, G. V. Ostrovskaya, Yu. I. Ostrovskiĭ, N. P. Tokarevskaya, A. G. Frank, A. Z. Khodzhaev, and N. N. Shedova, Pis'ma Zh. Tekh. Fiz. 1, 141 (1975) [Sov. Tech. Phys. Lett. 1, 68 (1975)].
[25]P. J. Baum, A. Bratenahl, and R. S. White, Phys. Fluids **16**, 226 (1973).
[26]P. J. Baum and A. Bratenahl, J. Plasma Phys. **11**, 93 (1974).
[27]P. J. Baum and A. Bratenahl, Laboratory Solar Flare Experiment, Report at the Flare Build-up Study Workshop, Falmouth, Cape Cod, Mass., USA., September 8–11 (1975).
[28]N. Ohyabu and N. Kawashima, J. Phys. Soc. Japan **33**, 496 (1972).
[29]N. Ohyabu, S. Okamura, and N. Kawashima, Phys. Fluids **17**, 2009 (1974).
[30]S. I. Syrovatskiĭ, Pis'ma Astron. Zh. 2, 35 (1976) [Sov. Astron. Lett. 2, 13 (1976)].
[31]S. I. Syrovatskiĭ, Vest. Akad. Nauk No. 3, 31 (1973).
[32]P. A. Sweet, Nuovo Cimento, Suppl. X. 8, 188 (1958).
[33]P. A. Sweet, in: Stellar and Solar Magnetic Fields (Ed. R. Lüst), Amsterdam, North-Holland (1965), p. 377.
[34]S. I. Syrovatskiĭ, in: Solar–Terrestrial Physics 1970, pt. 1, D. Reidel, Dordrecht (1972), p. 119.
[35]S. I. Syrovatskiĭ, Comm. Astrophys. and Space Phys. **4**, 65 (1972).
[36]S. I. Braginskii, in: Voprosy Teorii Plazmy (ed. M. A. Leontovich), Vol. 1, Moscow, Gosatomizdat (1963), p. 192; translated as: Reviews of Plasma Physics, Vol. 1, Consultants Bureau, New York (1965), p. 205.
[37]V. F. D'yachenko and V. S. Imshennik, Zh. Vychisl. Mat. Mat. Fiz. **3**, 915 (1963).
[38]A. A. Korchak and Yu. V. Platov, Astron. Zh. **45**, 1185 (1968) [Sov. Astron. 12, 939 (1969)].
[39]J. L. Culhane, J. F. Vesecky, and K. J. H. Phillips, Solar Phys. **15**, 394 (1970).
[40]S. I. Syrovatskiĭ and O. P. Shmeleva, in: Solar Terrestrial Relations; Proc. of the Conference held at the University of Calgary, Alberta, Canada, August 28–September 1, (1972), p. 243.
[41]O. P. Shmeleva and S. I. Syrovatskiĭ, Solar Phys. **33**, 341 (1973).
[42]O. P. Shmeleva and S. I. Syrovatskii, Pis'ma Astron. Zh. 2, 345 (1976).
[43]A. T. Wood, Jr., R. W. Noyes, A. K. Dupree *et al.*, Solar Phys. **24**, 169 (1972).
[44]A. T. Wood, Jr., and R. W. Noyes, Solar Phys. **24**, 180 (1972).
[45]B. V. Somov, Tr. Fiz. Inst. Akad. Nauk SSSR 88, 127 (1976).
[46]Z. Švestka, Solar Phys. **31**, 389 (1973).
[47]D. M. Rust, Y. Nakagawa, and W. M. Neupert, Solar Phys. **41**, 397 (1975).
[48]S. W. Kahler, J. F. Meekins, R. W. Kreplin, and C. S. Bowyer, Astrophys. J. **162**, 293 (1970).
[49]D. M. Horan, Solar Phys. **21**, 188 (1971).
[50]D. L. McKenzie, D. W. Datlowe, and L. E. Peterson, Solar Phys. **28**, 175 (1973).
[51]D. W. Datlowe, H. S. Hudson, and L. E. Peterson, Solar Phys. **35**, 193 (1974).
[52]K. P. Dere, D. M. Horan, and R. W. Kreplin, Solar Phys. **36**, 459 (1974).
[53]M. Landini, B. C. Monsignori Fossi, and R. Pallavicini, Solar Phys. **44**, 101 (1975).
[54]H. Zirin and K. Tanaka, Solar Phys. **32**, 173 (1973).
[55]R. L. Moore and D. W. Datlowe, Solar Phys. **43**, 189 (1975).
[56]F. M. Strauss and M. D. Papagiannis, Astrophys. J. **164**, 369 (1971).
[57]Yu. N. Starbunov and Yu. B. Chařikov, *in*: Tr. IV Leningradskogo Mezhdunarodnogo Seminara "Edinoobrazie Uskoreniya Chastits v Razlichnykh Masshtabakh Kosmosa," Leningrad (Proc. Fourth Leningrad International Seminar "Uniformity of Particle Acceleration on Different Scales in the Universe," Leningrad), Leningrad Institute of Nuclear Physics (1972), p. 145.
[58]W. T. Zaumen and L. W. Acton, Solar Phys. **36**, 139 (1974).
[59]K. A. Anderson, S. R. Kane, and R. P. Lin, in: Proc. of 3rd Leningrad International Seminar on Particle Acceleration on the Sun (Leningrad, 1970), Moscow, Moscow Univ. Press (1971), p. 269.
[60]J. C. Brown, Solar Phys. **18**, 489 (1971).
[61]S. R. Kane and R. F. Donnelly, Astrophys. J. **164**, 151 (1971).
[62]R. P. Lin and H. S. Hudson, Solar Phys. **17**, 412 (1971).
[63]H. Zirin, G. Pruss, and J. Vorpahl, Solar Phys. **19**, 463 (1971).
[64]S. I. Syrovatskiĭ and O. P. Shmeleva, Astron. Zh. **49**, 334 (1972) [Sov. Astron. **16**, 273 (1972)].
[65]D. M. Datlowe, M. J. Elcan, and H. S. Hudson, Solar Phys. **39**, 155 (1974).
[66]R. F. Donnelly, A. T. Wood, Jr., and R. W. Noyes, Solar Phys. **29**, 107 (1974).
[67]D. M. Horan, K. P. Dere, and R. W. Kreplin, Space Res. **14**, 441 (1974).
[68]J. R. H. Herring and I. J. D. Craig, Solar Phys. **28**, 169 (1973).
[69]I. J. D. Craig, Solar Phys. **31**, 197 (1973).
[70]W. M. Neupert, M. Swartz, and S. O. Kastner, Solar Phys. **31**, 171 (1973).
[71]W. M. Neupert, R. J. Thomas, and R. D. Chapman, Solar Phys. **34**, 349 (1974).
[72]K. J. H. Phillips, W. M. Neupert, and R. J. Thomas, Solar Phys. **36**, 383 (1974).
[72a]Yu. I. Grineva, V. I. Karev, V. V. Korneev, V. V. Krutov, S. L. Mandel'stam, U. I. Safronova, A. M. Urnov, L. A. Vainstein, and I. A. Zhitnik, Space Res. **15**, 637 (1975).
[73]K. G. Widing and Ch.-Ch. Cheng, Astrophys. J. **194**, L111 (1974).
[74]Ch.-Ch. Cheng and K. G. Widing, Astrophys. J. **201**, 735 (1975).
[75]K. G. Widing, *in*: Solar Gamma-, X-, and EUV Radiation (Ed. S. R. Kane), D. Reidel, Dordrecht–Boston (1975), p. 153.
[76]J. A. Vorpahl, E. G. Gibson, P. B. Landecker, D. L. McKenzie, and J. H. Underwood, Solar Phys. **45**, 199 (1975).

[77]J. A. Vorpahl, Astrophys. J. 205, 868 (1976).
[77a]I. P. Tindo, S. L. Mandel'shtam, and A. I. Shuryghin, Solar Phys. 32, 469 (1973).
[78]B. V. Somov, Solar Phys. 42, 235 (1975).
[79]J. Vorpahl and H. Zirin, Solar Phys. 11, 285 (1970).
[80]J. A. Vorpahl, Solar Phys. 26, 397 (1972).
[81]L. D. de Feiter, Space Sci. Rev. 16, 3 (1974).
[82]R. P. Lin, Space Sci. Rev. 16, 189 (1974).
[83]Z. Švestka, Ann. Rev. Astron. and Astrophys. 10, 1 (1972).
[84]A. A. Korchak, Astron. Zh. 44, 328 (1967) [Sov. Astron. 11, 258 (1967)].
[85]A. A. Korchak, Solar Phys. 18, 284 (1971).
[86]S. S. Holt and T. L. Cline, Astrophys. J. 154, 1027 (1968).
[87]R. L. Arnoldy, S. R. Kane, and J. R. Winckler, Astrophys. J. 151, 711 (1968).
[88]L. W. Acton, Astrophys. J. 152, 305 (1968).
[89]B. V. Somov, quoted in the collection,[8] p. 103.
[90]T. A. Chubb, R. W. Kreplin, and H. Friedman, J. Geophys. Res. 71, 3611 (1966).
[91]T. A. Chubb, quoted in the collection,[34] p. 99.
[92]J. C. Brown, in: Coronal Distrubances (IAU Symp. No. 57), (Ed. G. Newkirk, Jr.) D. Reidel, Dordrecht-Boston (1974), p. 395.
[93]S. W. Kahler, quoted in the collection,[75] p. 211.
[94]Solar Radio Group Utrecht, Space Sci. Rev. 16, 45 (1974).
[95]J. Fainberg and R. G. Stone, Space Sci. Rev. 16, 145 (1974).
[96]G. M. Simnett, Space Sci. Rev. 16, 257 (1974).
[97]J. C. Brown, quoted in the collection,[75] p. 245; A. A. Korchak, Astron. Zh. 53, 370 (1976) [Sov. Astron. 20, 211 (1976)].
[98]L. E. Peterson and J. R. Winckler, J. Geophys. Res. 64, 697 (1959).
[99]A. A. Korchak, Space Res. 13, 731 (1973).
[100]H. S. Hudson, in: High Energy Phenomena on the Sun (Eds. R. Ramaty and R. G. Stone), Greenbelt, GSFC (1973), p. 207.
[101]L. D. de Feiter, quoted in the collection,[75] p. 283.
[102]G. A. Stevens, Astron. and Astrophys. 31, 157 (1973).
[103]T. Takakura, quoted in the collection,[75] p. 299.
[104]D. W. Datlowe and L. E. Peterson, quoted in the collection,[6] Vol. 2, p. 291.
[105]H. F. Van Beek, L. D. de Feiter, and C. de Jager, Space Res. 14, 447 (1974).
[106]H. F. Van Beek, L. D. de Feiter, and C. de Jager, in: Correlated Interplanetary and Magnetospheric Observations (Ed. D. E. Page), D. Reidel, Dordrecht (1974), p. 533.
[107]J. C. Brown and P. Hoyng, Astrophys. J. 200, 734 (1975).
[108]P. Hoyng, Studies on Hard X-Ray Emission from Solar Flares and on Cyclotron Radiation from a Cold Magnetoplasma, Ph. D. Thesis (University of Utrecht, 1975).
[109]P. Hoyng, J. C. Brown, G. Stevens, and H. F. Van Beenk, quoted in the collection,[75] p. 233.
[110]J.-R. Roy and D. W. Datlowe, Solar Phys. 40, 165 (1975).
[111]D. W. Datlowe, quoted in the collection,[75] p. 191.
[112]J. C. Brown and A. N. McClymont, Solar Phys. 41, 135 (1975).
[113]L. D. de Feiter, quoted in the collection,[8] p. 93.
[114]S. I. Syrovatskiĭ: in: Solar Flares and Space Research, COSPAR Symposium (Eds. C. de Jager and Z. Švestka) D. Reidel, Dordrecht (1969), p. 346.
[115]S. Biswas and B. Radhakrishnan, Solar Phys. 28, 211 (1973).
[116]J. C. Brown, Solar Phys. 31, 143 (1973).
[117]Z. Švestka, Solar Phys. 13, 471 (1970).
[118]K. Najita and F. Q. Orrall, Solar Phys. 15, 176 (1970).
[119]R. P. Lin, quoted in the collection,[75] p. 385.
[120]J. C. Brown, Solar Phys. 36, 371 (1974).
[121]W. M. Glencross, Solar Phys. 29, 429 (1973).
[122]R. F. Donnelly and L. A. Hall, Solar Phys. 31, 411 (1973).
[123]S. R. Kane, Impulsive (Flash) Phase of Solar Flares-Hard X-Ray, Microwave, EUV and Optical Observations, Invited Review at IAU Symp. No. 57, Australia (1973).
[124]C. L. Hyder, G. L. Epstein, and R. W. Hobbs, Astrophys. J. 185, 985 (1973).
[125]K. A. Anderson and W. A. Mahoney, Solar Phys. 35, 419 (1974).
[126]R. V. Somov and S. I. Syrovatskiĭ, Solar Phys. 39, 415 (1974).
[127]V. Petrosian, Astrophys. J. 186, 291 (1973).
[128]J. C. Brown, Solar Phys. 26, 441 (1972).
[129]M. A. I. Van Hollenbecke, L. S. Masung, and F. B. McDonald, Solar Phys. 41, 189 (1975).
[130]M. A. Zel'dovich, B. M. Kuzhevskiĭ, I. A. Savenko, and I. A. Yudefovich, in: Issledovaniya Kosmicheskikh Lucheĭ (Investigations of Cosmic Rays), Nauka, Moscow (1975), p. 139.
[131]E. L. Chupp, D. J. Forrest, P. R. Higbie, A. N. Suri, C. Tsai, and P. P. Dunphy, Nature, 241, 333 (1973).
[132]E. L. Chupp, in: Trudy VI Leningradskogo Mezhdunarodnogo Seminara "Uskorenie Chastits i Yadernye Reaktsii v Kosmose," Leningrad (Proc. Sixth Leningrad International Seminar "Acceleration of Particles and Nuclear Reactions in the Cosmos," Leningrad), Leningrad Institute of Nuclear Physics (1974), p. 355.
[133]Zh. Verden, O. B. Likin, A. S. Melioranskiĭ, N. F. Pisarenko, I. A. Savenko, R. Talon, and V. M. Shamolin, Izv. Akad. Nauk SSSR, Ser. Fiz. 39, 272 (1975).
[134]A. S. Meliorensky, N. F. Pissarenko, W. M. Shamolin, O. B. Likin, R. Talon, G. Vedrenne, and B. Gourdon, Astron. and Astrophys. 41, 379 (1975).
[135]R. Ramaty and R. E. Lingenfelter, quoted in the collection,[75] p. 363.
[136]J. E. Vernazza, E. H. Avrett, and R. Loeser, Astrophys. J. 184, 605 (1973).
[137]P. S. MicIntosh and R. F. Donnelly, Solar Phys. 23, 444 (1972).
[138]M. E. Machado and D. M. Rust, Solar Phys. 38, 499 (1974).
[139]D. M. Rust and F. Hegwer, Solar Phys. 40, 141 (1975).
[140]T. Mathews and L. J. Lanzerotti, Nature 241, 335 (1973).
[141]H. S. Hudson, T. W. Jones, and R. P. Lin, quoted in the collection,[75] p. 425.
[142]E. L. Chupp, D. J. Forrest, and A. N. Suri, quoted in the collection,[75] p. 425.
[143]C. L. Hyder, Solar Phys. 2, 49, 267 (1967).
[144]C. L. Hyder, in: Mass Motions in Solar Flares and Related Phenomena, Nobel Symp. No. 9 (Ed. Y. Ohman) (1968), p. 57.
[145]Y. Nakagawa, S. T. Wu, and S. M. Han, Solar Phys. 30, 111 (1973).
[146]N. D. Kostyuk and S. B. Pikel'ner, Astron. Zh. 51, 1002 (1974) [Sov. Astron. 18, 590 (1975)].
[147]N. D. Kostyuk, Astron. Zh. 52, 752 (1975); 53, 361 (1976) [Sov. Astron. 19, 458 (1975); 20, 206 (1976)].
[148]Ya. B. Zel'dovich and Yu. P. Raĭzer, Fizika Udarnykh Voln i Vysokotemperaturnykh Gazodinamicheskikh Yavleniĭ, Ch. 12, §23 and 24; translated as: Physics of Shock Waves and High-Temperature Hydrodynamic Phenomena, Vols. 1 and 2, Scripta Technica, New York (1966, 1967).
[149]R. É. Guseĭnov, V. S. Imshennik, and V. V. Paleĭchik, Astron. Zh. 48, 1217 (1971) [Sov. Astron. 15, 968 (1972)].
[150]S. R. Pottash, Bull. Astron. Inst. Neth. 18, 7 (1965).
[151]R. McCray, R. F. Stein, and M. Kafatos, Astrophys. J. 196, 565 (1975).
[152]E. N. Parker, Astrophys. J. 117, 431 (1953).
[153]R. Weymann, Astrophys. J. 132, 452 (1960).
[154]G. B. Field, Astrophys. J. 142, 531 (1965).
[155]J. H. Hunter, Jr., Icarus 5, 321 (1966).
[156]Y. Nakagawa, Solar Phys. 12, 419 (1970).
[157]J. Schwarz, R. McCray, and R. F. Stein, Astrophys. J. 175, 673 (1972).
[158]D. P. Cox and W. H. Tucker, Astrophys. J. 157, 1157 (1969).
[159]F. Kneer and Y. Nakagawa, Astron. and Astrophys. 47, 65 (1976).
[160]R. F. Donnelly, Astrophys. J. 158, L165 (1969).
[161]R. Cruddace, F. Paresce, S. Bowyer, and M. Lampton, Astrophys. J. 187, 497 (1974).
[162]K. P. Dere, D. M. Horan, and R. W. Kreplin, quoted in the collection,[6] Vol. 2, p. 298.
[163]R. J. Thomas and R. G. Teske, Solar Phys. 16, 431 (1971).
[164]P. T. Kelly and W. A. Rense, Solar Phys. 26, 431 (1972).

Translated by Julian B. Barbour